ASSESSMENT OF RECENT DRIVERS OF CHANGE IN THE FLOW REGIME OF THE MULUNGUZI RIVER BASIN, MALAWI.

MASTER OF SCIENCE IN WATER RESOURCES MODELLING AND GOVERNANCE

THESIS

MUSSA CHING'AMBA

UNIVERSITY OF MALAWI

MAY 2024

ASSESSMENT OF RECENT DRIVERS OF CHANGE IN THE FLOW REGIME OF THE MULUNGUZI RIVER BASIN, MALAWI.

MSc (WATER RESOURCES MODELLING AND GOVERNANCE) THESIS

By

Mussa Ching'amba

BSc (Civil Engineering) –University of Malawi

Submitted to the School of Natural and Applied Sciences in partial fulfillment of the requirements for the Master's Degree (Water Resources Modelling and Governance).

UNIVERSITY OF MALAWI

MAY 2024

ABSTRACT

Watershed hydrology is primarily affected by Land Use/Land Cover (LULC) and climate change (CC). This study assessed the hydrological response of the Mulunguzi River Basin (MRB) to the impact of LULC and climate change between 1990 and 2020. Hydro-climate trends were analyzed using the Mann-Kendall method. The hydrological responses of the Mulunguzi watershed to various LULC and CC scenarios were quantified using the SWAT model. Based on the hydro-climatic analysis, it was found that the mean monthly and annual temperatures were consistently increasing by 0.004°C per month and 0.041°C per year. In addition, an increasing trend of 5.8mm per year was observed in rainfall. However, these trends were not statistically significant at a 95% confidence level. The decade of 2010-2020 experienced the highest amount of rainfall, totaling 9,529 mm, compared to the previous two decades of 1990-1999 and 2000-2009. According to the evaluation criteria, the SWAT model performance was satisfactory during calibration and validation, with respective Nash-Sutcliffe efficiency (NSE) of 0.59, coefficient of determination (R^2) of 0.62, and RSR of 0.64. NSE of 0.83, R^2 of 0.84, and observations standard deviation ratio (RSR) of 0.41. The SWAT results show that a reduction in the forested area of 24.04 % between 1990 and 2020 caused a 119.9% increase in surface runoff and a 17.8% decrease in base flow. With changes in rainfall and temperature, CC alone increased surface runoff, baseflow, evapotranspiration, and water yield by 152.2%, 33.6%, 19.1%, and 51.1 %, respectively. The combined impacts increased surface runoff and water yield by 303.8% and 71.2%, respectively. The study found that the combination of LULC alteration and CC led to more significant effects than that of either LULC or CC alone. These findings will provide valuable insights for effectively managing water resources, safeguarding the catchment area, and implementing climate change adaptation measures. This is critical because the water supply in Zomba City relies on the Mulunguzi catchment.

Keywords: Climate change; land use/land cover; Malawi; Mulunguzi River; streamflow; SWAT Model

DECLARATION

I, the undersigned, at this moment, declare that this thesis is my original work, which has not been submitted to any other institution for similar purposes. Where other people's work has been used, acknowledgments have been made.

_____

Full Legal Name

_____

Signature

_____

Date

CERTIFICATE OF APPROVAL/ CERTIFICATION

The undersigned certify that this thesis represents the student's own work and effort and has been submitted with our approval.

Signature: ----------Date: ----------

Cosmo Ngongondo**,** PhD (Professor)

Main Supervisor

Signature: ----------Date----------

Mwawi Kayuni, PhD

Programme Coordinator

DEDICATION

To my wife and two daughters (Tujaliwe and Upile) for enduring many days without my attention.

ACKNOWLEDGEMENTS

I am so grateful to God Almighty for enabling me to accomplish this work—special thanks to my supervisor, Professor Cosmo Ngongondo, for the guidance and assistance during my study. My sincere appreciation extends to Ms. Lusungu Nkhoma, PhD Candidate at the University of Oslo and the University of Malawi under the NORHED II supported project titled Climate Change and Ecosystems Management in Malawi and Tanzania (Project 3 #63826) for all the assistance with the SWAT modeling framework.

TABLE OF CONTENTS

ABSTRACT i
DECLARATION ii
CERTIFICATE OF APPROVAL/ CERTIFICATION iii
DEDICATION iv
ACKNOWLEDGEMENTS v
TABLE OF CONTENTS vi
LIST OF TABLES ix
LIST OF FIGURES x
ACRONYM AND ABBREVIATIONS xii
CHAPTER ONE 1
INTRODUCTION 1
1.1 Background Information 1
1.2 Problem Statement 3
1.3 Objectives of the study 4
1.3.1 The Main Objective 4
1.3.2 The Specific Objectives 4
1.4 The research questions 4
1.5 Hypothesis 4
1.6 Justification 4
1.7 Study Limitations 5
1.8 Thesis Arrangement 5
CHAPTER TWO 7
LITERATURE REVIEW 7
2.1 Introduction 7
2.2 Impacts of Land Use and Land Cover Change on water resources 10
2.3 Impacts of climate change on water resources 12
2.4 Combined impacts of LULC and climate change on water resources 13
2.5 Hydrological Models 15

2.5.1 Model Classification 15
2.5.2 Application of Hydrological Models 16
CHAPTER THREE 20
METHODOLOGY 20
3.1 The study area 20
3.2 Hydro-climatic Data Sources and Analysis 22
3.2.1 Trends in the hydro-climatic data 22
3.3 LULC Data sources and analysis 23
3.3.1 GIS and Remote Sensing in the Mulunguzi River Basin 23
3.3.2 Analysis of Land Use and Land Cover Changes. 25
3.3.3 Image Classification 26
3.4 Quantifying Impacts of LULC and Climate Change on Stream Flow 27
3.4.1 SWAT Model Data Input and Set-up 27
3.4.2 Data Preparation 27
3.4.3 Implementation of the SWAT model 28
3.4.4 Sensitivity Analysis 31
3.4.5 Calibration and Validation 33
3.4.6 Establishing Scenarios to Quantify the Impacts of Land Use and Climate Changes 34
CHAPTER FOUR 35
RESULTS AND DISCUSSIONS 35
4.1 Changes in Land Use and Land Cover from 1990 to 2020 35
4.2 Temporal Trends of the Hydroclimatology 38
4.2.1 Analysis of Temperature Trends 38
4.2.2 Rainfall 42
4.2.3 River Discharge Trends 48
4.3 The SWAT Model. 52
4.3.1 Sensitivity analysis 52
4.3.2 Calibration and Validation of the SWAT model 55
4.3.3 Impacts of Land Use and Climate Changes on Streamflow 62
CHAPTER 5 67
CONCLUSIONS AND RECOMMENDATIONS 67
5.1. Conclusions 67

5.2. Recommendations 69
REFERENCES 70
APPENDICES 74

LIST OF TABLES

TABLE 1 STATIONS FOR THE HYDRO-CLIMATIC DATA 22

TABLE 2 OBTAINING SATELLITE DATA FOR THE STUDY REGION. 23

TABLE 3. SELECTED PARAMETERS FOR SENSITIVITY ANALYSIS 32

TABLE 4 AREA AND PERCENTAGE OF LULC CLASSES IN THE MRB 35

TABLE 5 MANN KENDAL AND SEN'S SLOPE TEST RESULTS. 38

TABLE 6 MK RESULTS AND SEN'S SLOPE RESULTS 43

TABLE 7 SENSITIVITY ANALYSIS 53

TABLE 8 SUMMARY STATISTICS 56

TABLE 9 MEAN MONTHLY HYDROLOGICAL COMPONENTS FOR THE EFFECT OF LAND USE. 66

TABLE 10 MEAN MONTHLY HYDROLOGICAL COMPONENTS FOR THE EFFECT OF CLIMATE CHANGE. 66

TABLE 11 MEAN HYDROLOGICAL COMPONENTS FOR THE LULC AND CLIMATE CHANGE COMBINED EFFECT. 66

LIST OF FIGURES

FIGURE 1: STATUS OF MULUNGUZI DAM ON 18/12/2021. SOURCE: SRWB-PRO…….. **…..3**

FIGURE 2: LOCATION MAP OF MULUNGUZI RIVER BASIN……. ….21

FIGURE 3: MULUNGUZI RIVER BASIN…….. ...24

FIGURE 4: MULUNGUZI WATERSHED DELINEATION …….....28

FIGURE 5: SOIL MAP DEPICTING LITHOSOLS ……..30

FIGURE 6: SLOPE CLASSIFICATION ……..30

FIGURE 7: TIME SERIES PIE CHARTS FOR LULC **…….....36**

FIGURE 8: LAND USE AND LAND COVER CHANGE MAPS **…….....37**

FIGURE 9: MEAN ANNUAL TEMPERATURE FROM 1990-2020 **……39**

FIGURE 10: LINEAR TREND MEAN ANNUAL MAXIMUM TEMPERATURE …….....40

FIGURE 11: LINEAR TREND MEAN ANNUAL MINIMUM TEMPERATURE …….....41

FIGURE 12: ANNUAL RAINFALL TREND FROM 1990 TO 2020 ……44

FIGURE 13: TREND ANALYSIS WITHIN THE THREE DECADES ……45

FIGURE 14: TOTAL RAINFALL IN THE THREE DECADES …….....46

FIGURE 15: ANNUAL RAINFALL WITH PEAK YEARS …….....47

FIGURE 16: TREND OF STREAMFLOW AT MONTHLY SERIES …….....49

FIGURE 17: TREND OF STREAMFLOW AT ANNUAL SERIES ……..50

FIGURE 18: ANNUAL RAINFALL AND STREAM FLOW FOR MULUNGUZI WATERSHED ……51

FIGURE 19: GLOBAL SENSITIVITY ANALYSIS ……54

FIGURE 20: OBSERVED AND SIMULATED FLOWS DURING SWAT CALIBRATION……. …...57

FIGURE 21: OBSERVED AND SIMULATED FLOWS DURING SWAT VALIDATION. …….....57

FIGURE 22: MEAN MONTHLY DISCHARGE DURING THE CALIBRATION PHASE ……...….58

FIGURE 23: MEAN MONTHLY DISCHARGE DURING THE VALIDATION STAGE. ……...…..58

FIGURE 24: SCATTER PLOT OF THE OBSERVED AND SIMULATED MONTHLY AVERAGE FLOW (M3/S) IN THE CALIBRATION PHASE. ……..…59

FIGURE 25: SCATTER PLOT OF THE OBSERVED AND SIMULATED MONTHLY AVERAGE FLOW (M3/S) DURING THE VALIDATION PERIOD…….……... 60

FIGURE 26: FLOW DURATION CURVE OF OBSERVED AND SIMULATED DISCHARGE OF MULUNGUZI RIVER BASIN ……..61

ACRONYM AND ABBREVIATIONS

CC	Climate Change
DEM	Digital Elevation Model
DSMW	Digital Soil Map of the World
ESRI	Environmental Systems Research Institute
FAO	Food and Agriculture Organisation
GCMs	Global Circulation Models
GPS	Global Positioning System
HRU	Hydrologic Response Unit
ITCZ	Inter-tropical Convergence Zone
LULC	Land Use and Land Cover
MRB	Mulunguzi River Basin
MSS	Multispectral Scanner
NSO	National Statistics Office
OLI	Operational Land Imager
OLS	Ordinary Least Squares
SCS –CN	Soil Conservation Service - Curve Number Method
SRWB	Southern Region Water Board
SSURGO	Soil Survey Geographic Database of the US
SWAT	Soil and Water Assessment Tool Model
SGD	Sustainable Development Goals

TIRS	Thermal Infrared Sensor
USACE	United States Army Corps of Engineers
USGS	United States Geological Survey
UTM	Universal Transverse Mercator
WGS	World Geodetic System

CHAPTER ONE

INTRODUCTION

1.1 Background Information

Enhancing the availability of clean drinking water and proper sanitation is crucial for fulfilling Sustainable Development Goal 6 (SDG6). Most developing countries still face challenges in providing safe and adequate water (Cassivi et al., 2020). Rapidly increasing population is further stressing scarce freshwater resources (Kumambala, 2010). This, coupled with the effects of land use and land cover (LULC) alterations and CC (Climate Change), poses a significant challenge to the survival of water resources. Runoff and base flow are key water quantity indicators in catchments. Understanding the forces that drive them in watersheds supporting large populations is essential for water resource planning and development (Ngongondo, 2006). Alterations in LULC significantly impact the water balance in a watershed, affecting surface runoff, base flow, water yield, and evapotranspiration (Anaba et al., 2017; Osei et al., 2019). Climate change impacts the timing, volume, and peak water flows in ecosystems (Tan et al., 2015; Nkhoma et al., 2021).

Assessment of the alterations in LULC and CC effects on watersheds requires using methodologies that consider the unique characteristics of each watershed, such as its topography, LULC, climate, and hydrological aspects. For example, Tan et al. (2015) studied Malaysia's Johor River basin to investigate the isolated and collective effects of LULC alterations and CC. They found that methods like the paired catchment method, hydrological modeling, and statistical analyses helped understand the hydrological impacts of these changes. They particularly recommended hydrological modeling, as it effectively reveals the interaction among climate, land use, and hydrological dynamics. One of the models that has been applied extensively is SWAT (Soil and Water Assessment Tool Model). In Portugal, Carvalho-Santos et al. (2016) evaluated how land use and future climate conditions affect hydrology by employing the SWAT model. According to their study, climate change leads to lower flows during dry seasons and higher peak flows in wetter months. Bekele et al. (2021) applied the SWAT model to understand the hydrological response of Ethiopia's Keleta watershed to the effects of alterations in LULC. They observed significant land

alterations in the Keleta watershed from 1985 to 2010 reduced annual base flow while surface runoff and water yield increased.

Climate change has caused several challenges to water availability in many parts of Africa (Gautam, 2006). Nhemachena et al. (2020) argued that CC impacts are more adverse in Southern Africa. In this region, water stress and hydrologic variability have been exacerbated by increased warming conditions, variations in rainfall, and increased amount and occurrence of droughts and floods. Several studies across the region's major river basins suggest reduced water resources due to joint impacts of climate and LULC (Arora & Boer, 2001; Hamududu & Killingtveit, 2016). Studies have shown a decrease in runoff in the Zambezi River basin compared to other regions. A 10% reduction in precipitation was projected, which would correspondingly affect runoff. The study employed Global Circulation Models (GCMs) to project that the basin would be drier in 2100 (de Wit & Stankiewicz, 2006; Fant et al., 2015).

Nkhoma et al. (2021) studied southern Malawi, focusing on the Wamkurumadzi River, a Shire River tributary. It was concluded that CC had a greater influence on river flow than changes in LULC. The researchers emphasized the need for more integrated studies in Malawi's critical watersheds, considering alterations in LULC and CC. Kambombe (2018) conducted a study examining the impacts of climate variability in the Lake Chilwa Basin. The study focused on the sub-basins of Domasi, Likangala, Mulunguzi, and Thondwe rivers. The findings of the SWAT model in the Thondwe River Basin revealed that the combination of CC and land use modifications resulted in a 13% reduction in streamflow. In comparison, alterations in land use alone caused a 3% increase. Mbano et al. (2009) discovered that changes in runoff in the Mulunguzi catchment are mainly caused by CC rather than changes in LULC. Ngongondo (2006) also researched on the effects of variation in rainfall in the same catchment and found that a decline of 15% in long-term rainfall caused a 24% decrease in streamflow. These studies did not consider the joint effects of CC and alterations in LULC. Using the SWAT model, the present study research wishes to assess the hydrological response of the (Mulunguzi River Basin) MRB to the impacts of LULC and CC scenarios. This will provide insight into the causes of change in the flow of the Mulunguzi River, thereby enhancing our understanding of the region's hydrological dynamics.

1.2 Problem Statement

The MRB is a vital source of water for Zomba City. However, in recent times, the river's flow levels have reduced significantly in the dry season, particularly in the months leading up to the rainy season. This has resulted in dwindling water levels in the Mulunguzi Reservoir (Figure 1). Southern Region Water Board (SRWB), which manages water services in Zomba City, reports decreased water production during dry periods. There has been a notable reduction in forested areas within the catchment due to urbanization, increased deforestation, and agricultural land expansion (Dias, 2008). Besides changes in LULC, the catchment has also experienced variations in rainfall patterns and warmer climate conditions (Ngongondo, 2005). Previous studies in the Mulunguzi catchment have separately analyzed the impacts of LULC changes and CC on streamflow. However, these studies did not consider their combined impacts, which has left a gap in quantifying the hydrological response of the MRB to the joint effects of LULC changes and CC. This study aims to fill this critical knowledge gap, offering a more holistic view of the river's hydrological dynamics.

Figure 1: Status of Mulunguzi Dam on 18/12/2021. Source: SRWB-PRO

1.3 Objectives of the study

1.3.1 The Main Objective

The study's main objective was to assess the combined effects of LULC and CC on the river flow regime of the Mulunguzi River.

1.3.2 The Specific Objectives

Specifically, the study was aimed at:

i. Assessing the recent alterations in LULC in the MRB;
ii. Analyzing recent hydro-climatic trends in the catchment;
iii. Evaluating the isolated and combined effects of alterations in LULC and CC on river flow.

1.4 The research questions

The research seeks to address the following questions;

I. What are the alterations in LULC in the Mulunguzi catchment from 1990 to 2020?
II. What are the climatic trends in the MRB?
III. How do the changes in LULC, along with the effects of CC, affect the streamflow of the Mulunguzi River?

1.5 Hypothesis

The study was based on the null hypothesis that alterations in both LULC and Climate are significant drivers affecting Mulunguzi River flow patterns. The alternative hypothesis stated that the Mulunguzi River flow regime is predominantly influenced by either LULC change or CC.

1.6 Justification

Zomba City relies on the Mulunguzi River as its primary source of water. To address the water supply challenges in the city, which had affected the city, including the closure of institutions due to water shortages, the river was dammed under the National Water Development Project I (NWDP I) of the World Bank. The Mulunguzi Dam was built with a capacity of 3.4 Mm3. The population of Zomba City was 81,501, according to the 2008 population census. The 2018 Malawi Population and Housing Main Census Report indicated an increase of 23,512 from the 2008 population. The

Mulunguzi River has been negatively impacted by both LULC and climate change, regardless of the rise in population. It is imperative to comprehend the effects of CC and alterations in LULC on water resources such as the Mulunguzi River to manage the water supply efficiently and develop effective policies for water resource management.

1.7 Study Limitations

The study required daily climate data and observed flows for the Mulunguzi River. However, some daily values were missing from the climate data and observed flows. Furthermore, the other department with a station on the Zomba plateau did not provide the requested climate data.

1.8 Thesis Arrangement

Chapter 1: Introduction

The initial chapter of the research paper contains crucial contextual details regarding the requirement for evaluating the influence of LULC alterations and CC on the Mulunguzi River flow. The gaps in knowledge from previous studies regarding the hydrological components of the MRB are emphasized in the problem statement. The chapter also clearly outlines the objectives of the study.

Chapter 2: Literature Review

This chapter thoroughly examines the research background, focusing on the related literature. Studies and their methods for understanding the effects of alterations in LULC and CC are discussed in this section. Additionally, a literature review of hydrological models is presented in this section.

Chapter 3: Methodology

This section details the study area, data sources, and methodology to achieve objectives. It explains how the SWAT model was used, how LULC changes were quantified, and how hydro-climatic analysis was conducted.

Chapter 4: Results and Discussions

The study's findings are presented and analyzed in this chapter. The hydro-climatic analysis, LULC changes, and SWAT results have been discussed to quantify the hydrological components of the Mulunguzi River basin.

Chapter 5: Conclusions and Recommendations

This section highlights key research findings. Conclusions and recommendations have been made based on the results and discussions. The chapter also discusses the study's contribution to the management of water resources.

CHAPTER TWO

LITERATURE REVIEW

2.1 Introduction

Numerous researchers have studied the interrelated concepts of land use and land cover changes, seeking to understand their effects on various aspects, including water resources. land use pertains to the different ways in which humans make use of land and its resources, including agriculture, settlements, pasture, and recreation. Land use change refers to either a shift from one land utilization method to another or the intensification of an already existing land use. In contrast, land cover describes the natural and man-made features that exist on the land surface, including plants, structures, water bodies, and exposed areas. Alterations in land cover may involve changing from one type of land cover to another or modifying the state of a particular land cover classification. LULC change refer to the modifications that arise in the natural landscape due to both natural environmental factors and human activities (Turner and Meyer, 1994). Land Use and Land Cover (LULC) can have a significant impact on hydrological processes. When forest land is transformed into agricultural, urban, or bare land, it can lead to increased surface runoff and reduced infiltration. This is because the impervious surfaces created by such LULC changes result in reduced infiltration rates (Bekele et al., 2021). These changes in hydrological components may alter river flow regimes.

Climate change is primarily caused by the accumulation of greenhouse gases in the atmosphere. This accumulation results in the greenhouse effect, which causes global warming. As a result, global climate patterns change, leading to alterations in temperature and rainfall patterns worldwide (Li & Fang, 2021). According to the 2023 report by the Intergovernmental Panel on Climate Change, human activity is the main cause of climate change. Climate change has a direct impact on the hydrological cycle, affecting precipitation, evapotranspiration, soil moisture, and runoff. Intense and frequent rainfall can alter river flow, leading to flooding, while reduced river flow can be expected during droughts (Nhemachena et al., 2020).

The interplay among LULC, climate, and the hydrological cycle impacts river flow regimes. Watersheds face deteriorating water yields due to shifts in flow regimes. In 'The Natural Flow Regime,' Poff et al. (1997) described that changes in river flow display regional patterns influenced by climate and land cover, among other factors. The critical components of flow regimes were grouped into the discharge magnitude at any given interval, the rate of occurrence, the period related to specific flow conditions, the predictability of flows, and the rate of flow change. Naturally, river flows are derived from precipitation, surface runoff, and base flow (Poff et al., 1997). The two major environmental factors that affect flow regimes in watersheds are LULC and climate change. Therefore, understanding these factors is crucial in water resources management and catchment conservation.

Several studies have provided an understanding of the CC effects on streamflow. In one such study, Bekele and Knapp (2010) used a watershed model to investigate CC effects on water supply availability in the Chicago and Milwaukee metropolitan areas. The study found prolonged droughts caused water supply shortages during peak usage seasons. However, the research did not examine the crucial effects of population growth and water use patterns on water supply. Twisa and Buchroithner (2019) conducted a study in Tanzania's Wami basin, where they found that alterations in rainfall quantities and distributions affected water supply services. Mengistu et al. (2021) found increased runoff despite decreased precipitation in the Blue Nile River Basin. This paradoxical finding was attributed to the intensified occurrence of extreme rainfall events, offering a complex perspective on the relations between climate change and hydrological processes in the area.

LULC changes have been found to affect streamflow in numerous studies. Anaba et al. (2017) conducted a study in Uganda's Murchison Bay Catchment, where they observed that rapid LULC changes between 1997 and 2007 led to a significant increase in runoff, which was quantified at 26.73%. Between 1989 and 2002, land use in Malawi's Upper Shire River catchment changed significantly. During this time, there was a reduction in forested areas and savanna woodlands, while areas used for cultivation and grazing increased. These changes resulted in reduced base flow and increased surface runoff. The compounding effect was water scarcity during the dry season (Pullanikkatil, 2016).

In the past, studies on hydrological flow in watersheds mainly looked at the separate effects of LULC alterations and CC. However, recent research has highlighted the importance of considering the combined impact of both LULC alterations and CC (Belete et al., 2020; Malede et al., 2022). Different watersheds exhibit varied responses due to the distinct features of each watershed, including land cover, vegetation, topography, and the dominant climatic conditions. The effects of these factors differ from one watershed to another. Therefore, it is imperative to undertake studies considering these factors in individual watersheds to assess the current and future state of water resources (Serpa et al., 2015). Choukri et al. (2020) assessed the combined effects of alterations in LULC and CC on water availability in Northern Morocco. They used data-intensive simulation models to conclude that climate and land-use alterations caused water scarcity for both consumption and irrigation purposes.

The combination of LULC alterations and CC impacts has not been fully explored in previous studies conducted in the MRB. In 2009, Mbano et al. assessed the hydrological responses of the Mulunguzi and Namadzi catchments to the effects of CC and LULC alteration. Their findings suggested that in the Mulunguzi catchment, runoff was primarily determined by rainfall as opposed to changes in land cover. However, the study did not quantify the impacts due to the combination of alterations in LULC and CC, creating a gap in understanding how these interconnected factors influence watershed hydrology.

2.2 Impacts of Land Use and Land Cover Change on water resources

Land use and cover changes can significantly affect water flow within a watershed. For example, reducing forest coverage can lead to lower interception during rainfall, causing a rise in surface runoff. Changes in land use, particularly in agriculture and urban areas, can affect a watershed's hydrology by modifying infiltration, evapotranspiration, and groundwater recharge. These changes significantly impact the water yield and surface runoff in watersheds. Land use changes are frequently influenced by population growth and socioeconomic factors (Tesfaye et al., 2017).

In Iran's Anzali wetland catchment, Aghsaei et al. (2020) utilized the SWAT model to find that between 1990 and 2013, there was a 7% rise in agricultural land, which led to an increase of up to 8.3%, 7%, and 169% in evapotranspiration, water yield, and sediment yield, respectively. A reduction in these hydrological components was observed with an increase of 1.5% in urbanization. Deng et al. (2015) developed three LULC scenarios in 1980, 2000, and 2020. They used the Artificial Neuro Network model to simulate the 2020 LULC scenario and evaluated the hydrological processes using SWAT. The study predicted that rapid urbanization would cause a decrease in wood areas, grassland, and water areas by 2020. These changes in LULC would result in a notable increase in runoff into the Danjiangkou Reservoir. Furthermore, the annual runoff prediction showed non-uniformity in the runoff coefficient. It was concluded that runoff responded more to the impacts of LULC alterations than evapotranspiration. In a study by Khare et al. 2015, the SCS-CN model was utilized in the Narmada Basin to examine the effects of LULC alterations on the basin's runoff. LULC maps were developed for 1990, 2000, and 2009 using GIS and remote sensing. The study revealed that surface runoff increased by 10% between 1990 and 2009, which was influenced by the decrease in forestland and grassland by 6.7% and 20%, respectively, during the same period. These findings confirmed that alterations in LULC over time significantly impacted the basin's runoff.

Twisa et al. (2020) employed SWAT in the Wami River Basin to quantify the influence of distinct land use categories on hydrological elements in Tanzania. The alterations in LULC reduced forestland and increased cultivated land and urban areas. These changes increased surface runoff while decreasing the base flow and evapotranspiration in the Basin. In the Keleta watershed of Ethiopia, Bekele et al. (2021) found that the expansion of farmland and settlement at the expense of natural vegetation resulted in the increase of surface runoff and baseflow by 10.4% and 0.6%,

respectively, and a decrease in the baseflow by 3.5%. The changes from natural vegetation to farmland and settlement reduced the soil's infiltration capacity, leading to increased surface runoff and reduced groundwater flow. Various regional studies have used different models to predict how alterations in LULC affect hydrological components. Birhanu et al. (2019) conducted a study in the Gumara catchment of Ethiopia, using the HBV model and LULC maps from 1986, 2001, and 2015. The study found that between 1986 and 2015, there was a 13% increase in cultivated land and a 6% and 18% reduction in forest and grazing land, respectively. However, the results of the HBV model showed a minimal change of only ±5% in water balance components, indicating that the effects of LULC alterations on the hydrology of the Gumara catchment were not significant. The study attributed this observation to the HBV model's uncertainties and recommended using physically-based models.

Palamuleni et al. (2011) researched land cover alterations between 1989 and 2002 in the Shire River Catchment, Malawi. The results of the LULC analysis showed a 52% reduction in forest land, which was attributed to increased demand for firewood and timber. The reduction in the forest land increased grassland and build-up areas by 13% and 177%, respectively. Consequently, the SWAT model quantified reduced base flow and increased surface runoff. This resulted in water shortages during the dry season. These results confirm that alterations in LULC have adverse impacts on watershed hydrology.

2.3 Impacts of climate change on water resources

Greenhouse gas accumulation in the atmosphere is a primary contributor to climate change, as noted by Li and Fang in 2021. This phenomenon poses significant threats to water security in Southern Africa, affecting precipitation and evaporation patterns. Faramarzi et al. 2013 observed a decline in African water resources due to climate change, projecting extended dry periods, decreased rainfall, and increased annual variability. Similarly, Nhemachena et al. 2020 reported that climate change has led to warmer surface air temperatures, altered rainfall patterns, and more recurrent and intense droughts and floods.

A study by Arnell and Gosling (2013) assessed the impact of CC on global water resources. The study used Climate Model Intercomparison Project Phase 3 (CMIP3) and climate scenarios. The models showed that the mean annual runoff increased significantly across 26% of the global land area, mainly in South and East Asia. However, 27% of the global land area, particularly over Europe, the Mediterranean, South America, and Canada, showed a steady reduction in mean annual flow. Flood peaks increased in magnitude across 28% of the global land area, especially in Sub-Saharan Africa, even though a decreasing average annual runoff was also observed. Regarding temporal variability, the study found a one-month forward shift for the maximum mean monthly runoff. The study concluded that 47% of the land surface displayed increased annual runoff, 36% displayed decreased annual runoff, and 17% displayed a non-significant change. Following CC, streamflow prediction has become crucial in water resources planning and management. Li and Fang (2021) evaluated the effects of CC on streamflow in the Mun River Basin in Thailand. They used General Circulation (GCMs) and SWAT models. The study found that an increase of 1% in precipitation resulted in streamflow increases of 3.36%, 2.28%, and 2.34% under RCP2.6, RCP4.5, and RCP8.5, respectively. They also projected significant temperature increases across all RCPs, with more pronounced effects during the dry season, leading to reduced streamflow in that season. The effects of climate change vary from region to region. In the Cauto River of Cuba, Montecelos-Zamora et al. (2018) used SWAT to model hydrological responses to climate change. They utilized the regional climate model (RegCM4.3) to simulate the baseline data and used the RCP 8.5 emission scenario for future simulations. The study found that future climate projections between 2015 and 2039 showed an increase in average

annual temperature of 1.5°C and an 18% decrease in average annual rainfall. Consequently, the study found a reduction in streamflow compared to the baseline period.

In Africa, several studies have also tried to understand the impacts of CC on water resources. In the Kabompo River Basin in Zambia, Ndhlovu and Woyessa (2020) used GCMs and SWAT to model climate change impacts on the hydrology of the Basin. The study's findings indicate that there would be considerable increases in runoff, water yield, and rainfall under both RCP4.5 and RCP8.5. This suggested that climate change would cause significant alterations to the water balance components at different timescales. Similarly, Mengistu et al. (2021) utilized SWAT in conjunction with COSMO Climate Limited-area and regional climate models to investigate the effects of CC in the Abay River Basin of Ethiopia. The research revealed that precipitation decreased by -10.8% and -19.0% under RCP4.5 and RCP8.5, respectively. However, surface runoff increased by 7.6% and 13.6%. Despite the decrease in precipitation, the rise in surface runoff was attributed to the potential increase in rainfall intensity.

Adhikari and Nejadhashemi (2016) researched how the CC affects hydrological aspects in Malawi. The study was conducted in nine watersheds across Malawi. The study predicted an increase in the mean annual temperature in all the watersheds. However, precipitation predictions varied. The study projected a significant increase in mean annual rainfall in the Lake Chilwa Basin (which includes the MRB). The increase in rainfall signified a potential increase in evapotranspiration, soil moisture, surface runoff, and water yield. This study demonstrated the hydrological responses of Malawi's watersheds to the effects of CC.

2.4 Combined impacts of LULC and climate change on water resources

Alterations in LULC have a vital influence on watershed hydrology, which CC further compounds. The impacts are substantial and evident in different aspects, such as surface runoff, base flow, evapotranspiration, and water yields in watersheds (Kumar et al., 2022). Climate changes caused by global warming affect the timing and distribution of rainfall and the frequency and intensity of floods, recharge of groundwater, and surface runoff (Yang et al., 2017). However, the extent of these impacts varies across different watersheds. There is a divergence in scholarly opinion regarding whether LULC change or climate change exerts a more significant influence on watershed hydrological components, as noted by Malede et al. (2022). Thus, there is a growing

need to carry out investigations combining the impacts of LULC changes and CC on the various hydrological elements.

Recent studies at a global scale have applied various models to quantify the effects of LULC alterations and CC on water resources. In India, Kumar et al. (2022) evaluated the hydrological response of the Usri watershed to the integrated effects of alterations in LULC and CC. The results of the SWAT model showed a significant increase in stream flow across three distinct periods (1985-1995, 1996-2006, and 2006-2016), primarily due to the combined impact of urbanization and rainfall. The research concluded that the combination of alterations in LULC and CC has a more significant impact on hydrological components than either of these factors on their own. Other scholars have stressed the need to separate the effects of alterations in LULC from that of CC when conducting studies considering both factors. For example, Li et al. (2009) conducted a study to examine the effects of alterations in land use and CC on surface runoff, baseflow, and evapotranspiration in the Loess Plateau Catchment of China. The study considered the individual contributions of either land use alterations or CC. The study found that between 1981 and 2000, the catchment underwent a change of 4.5% from shrubland and woodland to grassland. The catchment also experienced a decrease in precipitation of about 18% and an increase in temperature of 6 °C. The SWAT model results showed a 9.6% and 18.8% decrease in runoff and 95.8% and 77.1% decrease in soil water content. Land use alterations increased evapotranspiration by 8%, while CC caused a decrease of 103%. The study concluded that CC had a more significant impact on the catchment's hydrology than the changes in LULC.

Although the hydrological effects of LULC alterations and CC happen globally, conducting studies at regional and local scales is essential because hydrological response of watersheds vary depending on local climate, geographical features, soil type, and vegetative cover. Malede et al. (2022) studied Ethiopia's Birr River Watershed to investigate the impact of alterations in LULC and CC on hydrological flows. To identify significant variations in surface runoff, they used the SWAT model. Their findings revealed that between 1986 and 2018, agricultural land and settlement increased by 25% and 55%, respectively, while forest land decreased by 61%, bushland by 26%, and grassland by 39%. The study showed that surface runoff increased by 90% and 13% in 1997–2007 and 2008–2018, respectively, due to the combined effects of land use alterations and CC. Baseflow increased by 14% between 1997 and 2007 but decreased by 8% between 2008

and 2018. It was concluded that surface runoff was more sensitive to the combined effects of LULC alterations and CC than their individual effects.

In Malawi, Nkhoma et al. (2021) studied the Wankurumadzi River Basin to examine the impacts of CC and LULC alterations on the stream flow. The SWAT results showed that the mean annual discharge decreased by 44.48% from the 1980s to the 1990s and then increased by 113.3% from the 1990s to the 2000s. There was a 1.6% increase in the average river discharge from the 1980s to the 2000s. The study also analyzed the rainfall patterns and found that the Wankurumadzi River Basin is highly sensitive to rainfall variability. The 2000s had more rainfall compared to the 1990s, which suggests that rainfall is a critical factor in the Wankurumadzi River's hydrological response.

2.5 Hydrological Models

Many studies have used different hydrological models to examine how watersheds respond to LULC and climate change. According to Sorooshian (2008), these models represent natural environmental systems. Meteorological data, topographical information, soil properties, and land use patterns are usually used as inputs for these models. Devia et al. (2015) explain that hydrological models serve different purposes, such as flood prediction, streamflow estimation, drought investigation, water quality evaluation, water resource management, and CC impact analysis.

2.5.1 Model Classification

Hydrological models are categorized based on diverse criteria. Spatial representation is one such criterion, according to Sorooshian (2008). Lumped, distributed, and semi-distributed models can be grouped under this criterion. Lumped models consider the modeled area as a whole and employ average parameter values for the entire area. They are relatively easy to create. However, they are not effective in capturing spatial variability. Distributed models divide the modeled area into grid cells to capture spatial variability. These models require detailed spatial data. Semi-distributed models group areas based on similar characteristics. Models are also classified as stochastic and deterministic. Each time a stochastic model is run with a specific input, a different output is generated, and both the input and output are regarded as random variables. On the contrary, a deterministic model is designed to yield identical results when given a particular set of inputs every time. Devia et al. (2015) suggested a classification system for hydrological models based on their

temporal focus. The models were divided into two categories: event-based and continuous models. The former is intended to simulate specific hydrological events, such as floods, while the latter is better equipped to simulate hydrological processes over extended periods. In 2008, Sorooshian put forth an alternative approach to classifying hydrological models. His classification system was based on the process description method used by models, which he divided into three categories: empirical models, conceptual models, and physically based models. Empirical models rely on statistical relationships derived from historical data and do not explicitly represent the underlying physical processes, hence the black box models. Physically based models, conversely, simulate hydrological processes grounded in physical laws and principles, offering a more detailed and mechanistic understanding of hydrological phenomena. Conceptual models represent a middle ground, providing simplified portrayals of physical processes. They blend theoretical understanding with empirical insights, making them less abstract than theoretical models yet more grounded in physical reality than purely empirical models.

2.5.2 Application of Hydrological Models

Hydrological models are created for various purposes. Several research studies have employed MIKE SHE, VIC, HEC-HMS, and SWAT models to evaluate how LULC and climate change affect water resources.

2.5.2.1 MIKE SHE (Systeme Hydrologique European)

This is a physically distributed model that considers different hydrological cycle components. This includes precipitation, evapotranspiration, interception, river flow, and groundwater flow. The model requires data such as Digital Elevation Models, soil characteristics, climatic data, groundwater information, surface water details, and data on human activities such as irrigation practices to create an accurate simulation. The model mainly simulates groundwater and surface water dynamics and recharge processes. Wang et al. (2013) conducted a study that utilized the MIKE SHE model to assess CC and LULC alterations effects on streamflow in the Chaohe watershed in China. The study revealed that between 1980 and 1989, changes in flow were contributed by CC and alterations in LULC by 51% and 49%, respectively. Between 2000 and 2008, CC had a more dominant role, contributing 78% to flow changes, compared to 22% from LULC changes. Although the MIKE SHE model provides comprehensive insights into hydrological processes, it has a complex setup and requires extensive data, making it

computationally demanding. Additionally, as noted by Singh and Frevert (2006), the MIKE SHE model is not freely available, as it is a commercial product, which may limit its accessibility for some users.

2.5.2.2 VIC (Variable Infiltration Capacity model) model.

The VIC model uses water and energy balance equations at each grid cell to simulate infiltration, surface runoff, and base flow (Hengade, 2019). The model data input includes temperature, wind speed, precipitation, land cover types, and soil characteristic parameters (Cuo et al., 2013). The hydrological response of watersheds to alterations in LULC and CC has been assessed extensively using the VIC model. In India, Hengade (2019) employed the VIC model to assess the hydrological response of the Godavari River basin to the effects of alterations in LULC and CC. The study concluded that hydrology was affected more by CC than by changes in land cover. The VIC model is particularly suitable for simulating hydrology in cold regions as it can incorporate frozen soil and snow accumulation characteristics. However, it is not recommended for small watersheds and is most applicable in moist areas and agricultural domains (Cuo et al., 2013).

2.5.2.3 HEC-HMS (Hydrologic Engineering Center-Hydrologic Modeling System)

United States Army Corps of Engineers (USACE) created HEC-HMS, a modeling system designed to imitate dendritic watershed systems' rainfall-runoff and routing processes. Meteorological data (which includes rainfall, temperature, and evapotranspiration), watershed characteristics (DEM, LULC, and soil characteristics), and hydrologic parameters (including river and stream network, reservoir and lake data, channel parameters, and flow routing parameters) are necessary inputs for the model (Msaddek et al., 2020). Flood hydrology analysis, river basin water supply, and watershed runoff are among the primary uses of the HEC-HMS model (Fleming, 2004). Koneti et al. (2018) examined the LULC effects on streamflow patterns in the Godavari River Basin in India. The HEC-HMS model showed that deforestation and increased agricultural land resulted in more significant runoff and less evapotranspiration in the basin. Although the HEC-HMS model visually represents outcomes, it is more suitable for simulating flood events and issuing stormwater warnings rather than predicting hydrological changes over extended periods (Bai et al., 2019).

2.5.2.4 *SWAT* model (Soil and Water Assessment Tool)

The study selected the SWAT model over other models due to its data input requirements. The SWAT model can simulate weather data such as solar radiation and wind speed, which is not comprehensively available. Additionally, the model is applicable in small watersheds and is not computationally demanding. It is freely available and does not limit accessibility to its users.

This model is process-based and semi-distributed, can be adapted to different scenarios, and is freely available. Mekonnen et al. (2017) employed SWAT to quantify the hydrological response of the Upper Blue Nile River Basin to LULC and CC impacts. Their findings indicated a 16% increase in streamflow from the 1970s to the 2000s due to these combined impacts. Similarly, Nyatuame et al. (2020) conducted a study in the Tordzie watershed, covering an area of 1278.3 km^2, and found that LULC changes significantly impacted the watershed's hydrology.

The SWAT model's detailed handling of climate and LULC change makes it critical in these studies. Arnold et al. (2012) stated, “The SWAT model has two main phases. The first phase is the land phase, which considers water, sediment, nutrients, and pesticide loadings to the main channel in each sub-basin. The second phase is the routing phase, which calculates water flow through channels and between basins.” The land phase uses the water balance method ($SWt = SW0 + \sum ti=1 + (Rv – Qs – Wseepage – ET – Qgw)$), which involves soil humidity, rainfall volume, surface runoff, soil water seepage, evapotranspiration, groundwater runoff, and time.

Model input data include watershed characteristics (consisting of LULC maps, DEM, and soil maps), climatic data (encompassing rainfall, temperature, solar radiation, relative humidity, and wind speed), and observed flows. Sensitivity analysis uses ArcSWAT tools to determine model calibration and validation parameters. During the analysis, multiple simulations are conducted by SWAT. Various calibration algorithms in the SWAT CUP program, including GLUE, SUFI2, ParaSol, and MCMC, were created by Abbaspour et al. (2012). Rainfall-runoff modeling typically uses SUFI2 for calibration.

Once calibration is completed, the model validation stage follows, which involves evaluating the consistency of the simulation using various metrics. According to Moriasi et al. (2007), these metrics are used to measure the accuracy of a model: the "Nash Sutcliffe Efficiency" (NSE), which measures the model's accuracy; the "Root Mean Square Error-Observations to Standard Deviation Ratio" (RSR) which compares the average tendency of simulated data to observed data, the

"Coefficient of Determination" (R^2) which quantifies the correlation between simulated and observed data, and the "Percent of Bias" (PBIAS) which compares the average tendency of simulated data to observed data.

The hydrological components of watersheds are dependent on both LULC changes and CC. LULC changes such as deforestation or urbanization, increase surface runoff and chnage river flows. Conversely, CC affects the hydrological cycle by altering precipitation, evapotranspiration, and soil moisture. Previous studies have emphasized examining the combined effects of LULC changes and CC on streamflow and water resource management, which forms a comprehensive basis for addressing knowledge gaps in the Mulunguzi Catchment area by focusing on the interlinkages between LULC and CC. Various hydrological models, such as SWAT, MIKE SHE, and VIC are applied to predict the impacts of LULC changes and CC on different watersheds. Localized research is essential for effective water resource management due to the unique environmental characteristics of each watershed.

CHAPTER THREE

METHODOLOGY

3.1 The study area

The Mulunguzi River Basin is within the Lake Chilwa Basin in Southern Malawi. It is positioned between latitudes of 15° 22′ 0″ S and 15° 55′ 0″ S and longitudes of 35° 15′ 0″ E and 35° 20′ 30″ E (Figure 2). The Lake Chilwa Basin covers a total area of 8,349 km², with 68% in Malawi and 32% in Mozambique. The Mulunguzi River Catchment is located exclusively on Zomba Mountain, 1800 meters above sea level. It covers an area of roughly 19.2 km², as Mbano et al. (2009) reported.

Zomba Mountain is a high-relief area that receives high rainfall, with mean annual rainfall reaching 2000mm. Ngongondo (2005) reported maximum and minimum rainfall of 3,179mm in 1978 and 1,059 mm in 1991, respectively, between 1954 and 2003. The primary rain-bearing system in the area is the Inter-tropical Convergence Zone (ICTZ), which experiences occasional cyclonic rainfall activities. The rainfall months in the region begin from November to April, with the maximum rainfall recorded in January or February (Ngongondo, 2005).

The porphyritic quartz microsite characterizes the inner ring of the Zomba mountain massif. Due to frequent rainfall and intense weathering, the syenites transform into deep-red brown silty clay soil. On the steeper inclines of the Mulunguzi Valley, the soil profile is compacted with rounded boulder debris and heavily eroded syenite fragments that often shift due to gravity-induced sediment movement (Dias, 2008). The main land cover in the Mulunguzi catchment is Pinus and Widdringtonia species under the forest plantation. Within the plantation, there are also woodlots of Eucalyptus. The pine plantation occupies an area of about 75%. The first Pinus Patula trees were planted in 1920.

The catchment has the Mulunguzi dam, which has a capacity of 3.4Mm^3. The city of Zomba, with a population of 105,013, relies solely on the Mulunguzi Dam for its water supply (NSO, 2019). In

addition to water supply, the Mulunguzi Catchment also supports fishing, agricultural, and tourism activities (Mbano et al., 2009).

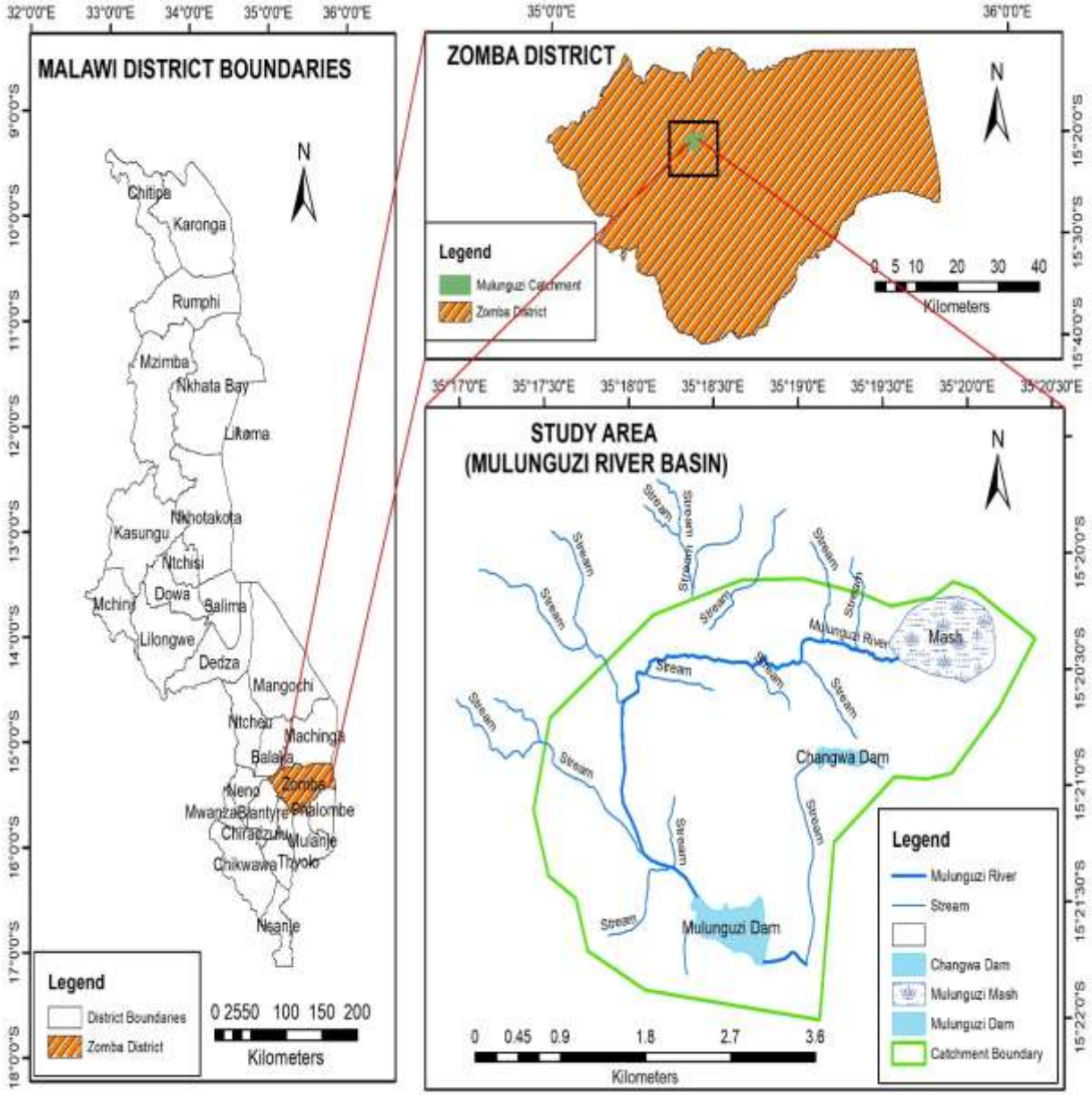

Figure 2: Location Map of Mulunguzi River Basin

3.2 Hydro-climatic Data Sources and Analysis

Daily weather data, such as precipitation, temperature, and hydrological data, were utilized in the research. The 'Malawi Department of Climate Change and Meteorological Services,' Climate Hazard Group Infrared Precipitation with Station data (CHIRPS), and POWER (NASA's Prediction of World-Wide Energy Prediction) were the sources of the climatic data. CHIRPS and POWER were used to estimate Areal rainfall and temperature, respectively. The hydrological data was sourced from the 'Malawi Department of Water Resources.' Table 1 provides a summary of the metadata and record length.

Table 1 Stations for the Hydro-climatic Data

Data Source/Station	Latitudinal (S)	Longitudinal (E)	Elevation (m)	Period	Type
Chancellor College	-15.38	35.35	886	1990-2020	Meteorological
Kuchawe Met	-15.3	35.31	1300	1990-2020	Meteorological
CHIRPS	-15.35	35.32	900	1990-2020	Meteorological
POWER	-15.35	35.32	891	1990-2020	Meteorological
Mulunguzi (20208)	-15.21	35.18	980	1990-2020	Hydrological

3.2.1 Trends in the hydro-climatic data

The data was analyzed for trends using the Mann-Kendall (MK) test statistic, which is a non-parametric method developed by Mann (1945) and Kendall (1975). A significance level of $\alpha=0.05$ was used. The World Meteorological Organization (WMO) recommends using MK to detect monotonic trends in hydro-meteorological variables (WMO, 1988). MK is the preferred method for non-normally distributed data like rainfall as it is not affected by missing data or outliers (Ngongondo et al., 2011). To estimate the magnitudes of the significant trends (slopes), Sen's slope method (Sen, 1968; Hirsch et al., 1982) was employed.

3.3 LULC Data sources and analysis

The LULC database for the Mulunguzi catchment was created by utilizing Landsat TM images downloaded from the United States Geological Survey (USGS) platform. Image acquisition details are summarized in Table 2.

Table 2 Obtaining Satellite Data for the Study Region.

Source	Sensor	Path/Row	Spatial Resolution	Acquisition Date
Earthexplorer.usgs.gov	Landsat 1-5 TM	167/71	30m x 30m	April, 1990
	Landsat 4-5 TM	167/71	30m x 30m	May, 2000
	Landsat 8 ORI	167/71	30m x 30m	May, 2020

3.3.1 GIS and Remote Sensing in the Mulunguzi River Basin

GIS and remote sensing were used to map crucial features of the MRB. Figure 3 displays the basin produced in ArcMap. The study required identifying critical features in the basin, including streams, rivers (such as the Mulunguzi River), the Chagwa Dam, the Mulunguzi Dam, and the Mulunguzi Mash. These features were crucial for the SWAT modeling and LULC change analysis.

The first task was data acquisition. The handheld GPS collected data points for streams, rivers, dams, and mash. During this exercise, ground truth data for LULC classes were also collected. This data was essential during LULC mapping (a detailed explanation is given in section 3.3). Satellite images used to produce the LULC map were downloaded from the USGS website. After data acquisition, processing was conducted in ArcMap.

In the ArcMap, points representing streams and rivers were connected as polylines. Points for Mulunguzi Dam, Chagwa Dam, and Mulunguzi Mash were mapped as polygons. The polygons represent the boundaries of these features. The polylines and the polygons give a better visualization and an accurate representation of features in the Basin. A classified satellite image was integrated into the mapped features to complete the Map for the Mulunguzi River Basin (image classification is detailed in section 3.3.3).

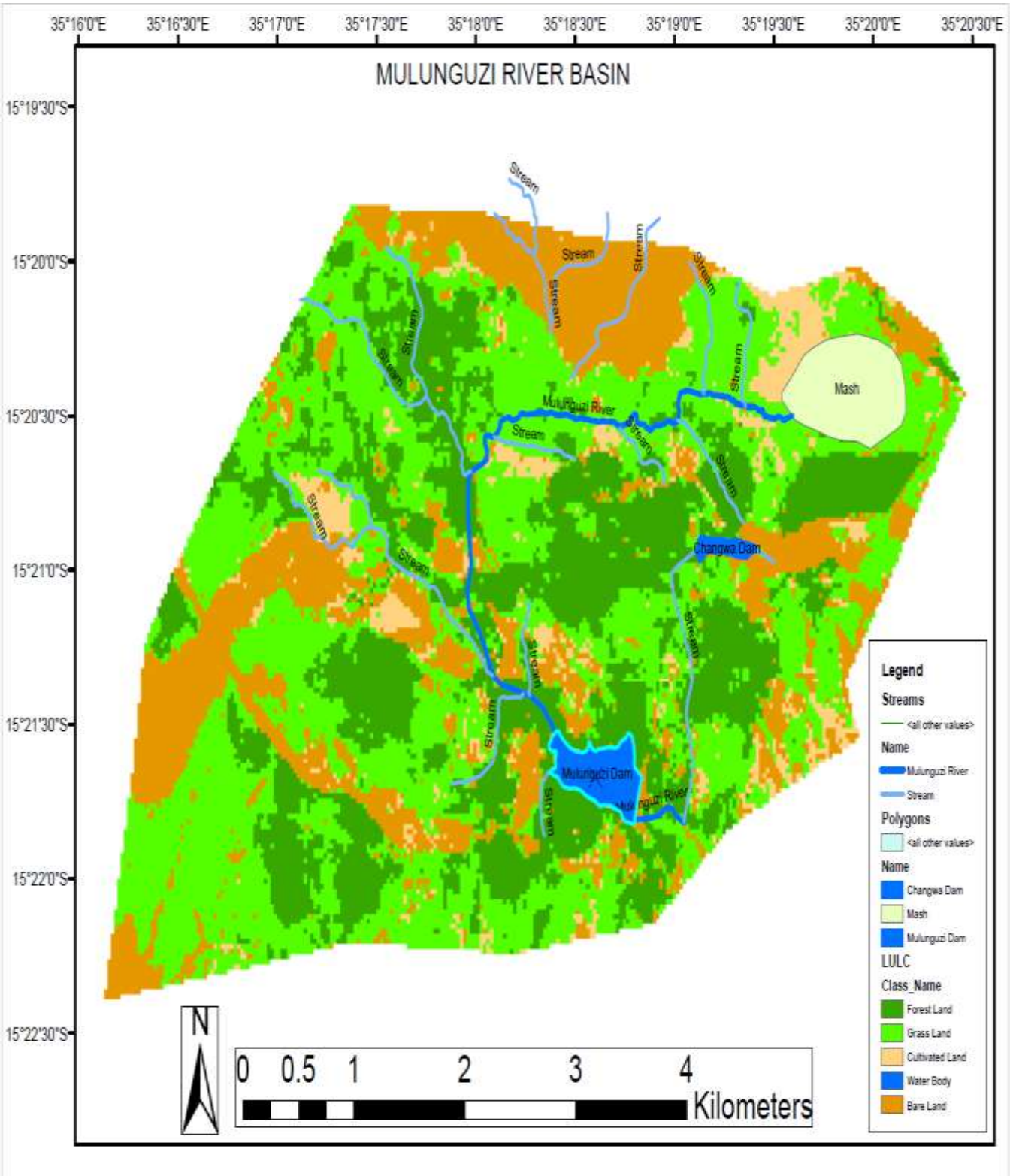

Figure 3: Mulunguzi River Basin

3.3.2 Analysis of Land Use and Land Cover Changes.

GIS and remote sensing measured LULC alterations between 1990 and 2020. This method has been applied in various research studies, such as Malede et al.'s (2022) study in the Abbay Basin, Ethiopia; Nkhoma et al.'s (2021) study in the Wamkurumadzi Basin, Malawi; Kambombe's (2018) study in the Lake Chilwa Basin, Malawi; Tan et al.'s (2015) study in the Johor River basin, Malaysia; and Pullanikkatil et al.'s (2016) study in the Likangala River catchment in Zomba, Malawi.

3.3.2.1 Image Preprocessing

Before conducting change detection, it is crucial to preprocess the images. The acquired images underwent preprocessing to establish a more precise link between the image and the actual biophysical occurrence, correct errors that arose during data collection, and remove any image noise (Coppin et al., 2004). The ArcMap 10.5, developed by ESRI, was used for preprocessing. Geometric correction, masking, band composite, and extraction were among the preprocessing techniques used in ArcMap.

3.3.2.2 Geometric correction

All the collected images underwent geometric correction to minimize the impact of sensor errors. Subsequently, they were projected onto the Universal Transverse Mercator (UTM) system, the standardized coordinate system used in Malawi (Pullanikkatil, 2016). The projection was specifically carried out in Zone 36S, WGS 84.

3.3.2.3 Masking

The presence of clouds in satellite imagery may obscure important features of interest. The masking tool in the ArcMap was used to remove cloud-covered areas in the images (Jensen, 2015)

3.3.2.4 Band Composite

The downloaded images contained several bands which captured different wavelengths of light. Each band represented different information about the surface of the earth. Combining different spectral bands from satellite imagery creates a band composite, which helps distinguish specific features on the Earth’s surface. Therefore, a distinct band composite represents each land cover type (Jensen, 2015). Similar to Pullanikkatil (2016), the Near Infrared (NIR), Red, and Green

bands were combined to create a false color composite that highlights vegetation (Band 5, Band 4, and Band 3). Healthy vegetation reflects a lot of NIR, which produces a bright or dark red color for forested areas. Grassland, conversely, reflects less near-infrared since grasses are shorter and less dense than trees. Hence, they appear light red or pinkish compared to the forest. Agricultural land appears in varying shades of red, but they have a distinct rectangular pattern that signifies planted fields. NIR, green, and blue bands were combined to identify water bodies. In this color composite, water bodies appear black, which makes them stand out from other land cover types (Band 5, Band 3, and Band 2). Bare land areas can be efficiently highlighted by combining NIR, Red, and Short-Wave Infrared (Band 5, Band 4, and Band 7). In this color composite, bare land appears distinctly brown or grey (Jensen, 2015).

3.3.3 Image Classification

A supervised classification method was utilized to classify pixels into various LULC types in a raster dataset. This was accomplished by using the Spatial Analyst Tool available in ArcMap. The Mulunguzi Watershed was categorized into five different LULC classes - Forest Land, Grassland, Agricultural Land, Bare Land, and Water Bodies. The dominant land cover, insights gained from GIS watershed mapping, and extensive literature review were the factors used to establish these categories (Kambombe, 2018; Pullanikkatil et al., 2016; Dias, 2008). Training samples were required for the LULC classes, which were selected by drawing polygons in identified and selected areas within the images that represented a known LULC class. Based on the training samples, a spectral signature file was created containing the mean digital numbers of each band for every class represented in the training samples. Once the signature file was ready, the image was classified using ArcMap's “Maximum Likelihood Classification” algorithm (Jensen, 2015).

3.4 Quantifying Impacts of LULC and Climate Change on Stream Flow

In examining the effects of LULC and climate change on streamflow, the research utilized the SWAT model and ArcSWAT-2012 extension in ArcGIS 10.5. Calibration and validation of the model were performed using the SWAT-CUP tool.

3.4.1 SWAT Model Data Input and Set-up

The necessary model input data were the LULC map, soil map, Digital Elevation Model (DEM), and hydro-meteorological data. The Mulunguzi River basin was divided into sub-basins through catchment delineation, further segmented into Hydrological Response Units (HRUs). Based on the land cover, soil types, and slope classes, each Hydrologic Response Unit (HRU) was categorized. This methodology is comparable to the one utilized by Serpa et al. (2015).

3.4.2 Data Preparation

LULC maps were produced for 1990, 2000, and 2020 using ArcMap, as described in section 3.3 of the study. The Food and Agriculture Organization (FAO) website provided the soil map (www.fao.org/geonetwork). The Soil Map of the world was downloaded and then imported into ArcMap. This allowed the extraction of the Zomba soil map using the Zomba shape file. Creating an accurate representation of the soil in the specific study area required further refinement of the soil map using the shape file of the study area. The LULC and soil maps were assigned grid values based on their respective classifications and types. The maps were initially projected onto the WGS84 UTM Zone 36S coordinate system and later converted into raster files for integration into ArcSWAT. The United States Geological Survey (USGS) website provided a Digital Elevation Model (DEM) with a spatial resolution of 30 meters. A DEM was customized to the study area by using its shape file.

The study utilized meteorological data from 1990 to 2020, including daily rainfall records and the minimum and maximum temperatures. Where data was missing, a value of -99.00 was inserted as a placeholder to indicate the absence of data within ArcSWAT. Additionally, other weather parameters, such as solar radiation, wind speed, and relative humidity, were created by the ArcSWAT tool. The calibration and validation of the SWAT model were conducted using streamflow data obtained from the Mulunguzi gauging station. This data was instrumental in refining the model to represent the hydrological processes within the study area.

3.4.3 Implementation of the SWAT model

The data inputs outlined in section 3.6.2 were used to develop the SWAT model. In Arc SWAT, a new project was created, and the subsequent steps were taken:

3.4.3.1 Watershed Delineation.

The DEM was imported into the SWAT program to calculate the flow direction and its accumulation. The total area calculated was 35.9 hectares, consisting of 400 cells. Next, the drainage network was created by the program. Subsequently, the watershed was delineated, and sub-basins were defined. As per the method detailed by Abbaspour et al. (2012), hydrological response units (HRUs) were also established. The topographic report showed that the watershed had a minimum elevation of 1330m and a maximum height of 2049m. The delineated watershed produced 30 reaches and sub-basins, as seen in Figure 4.

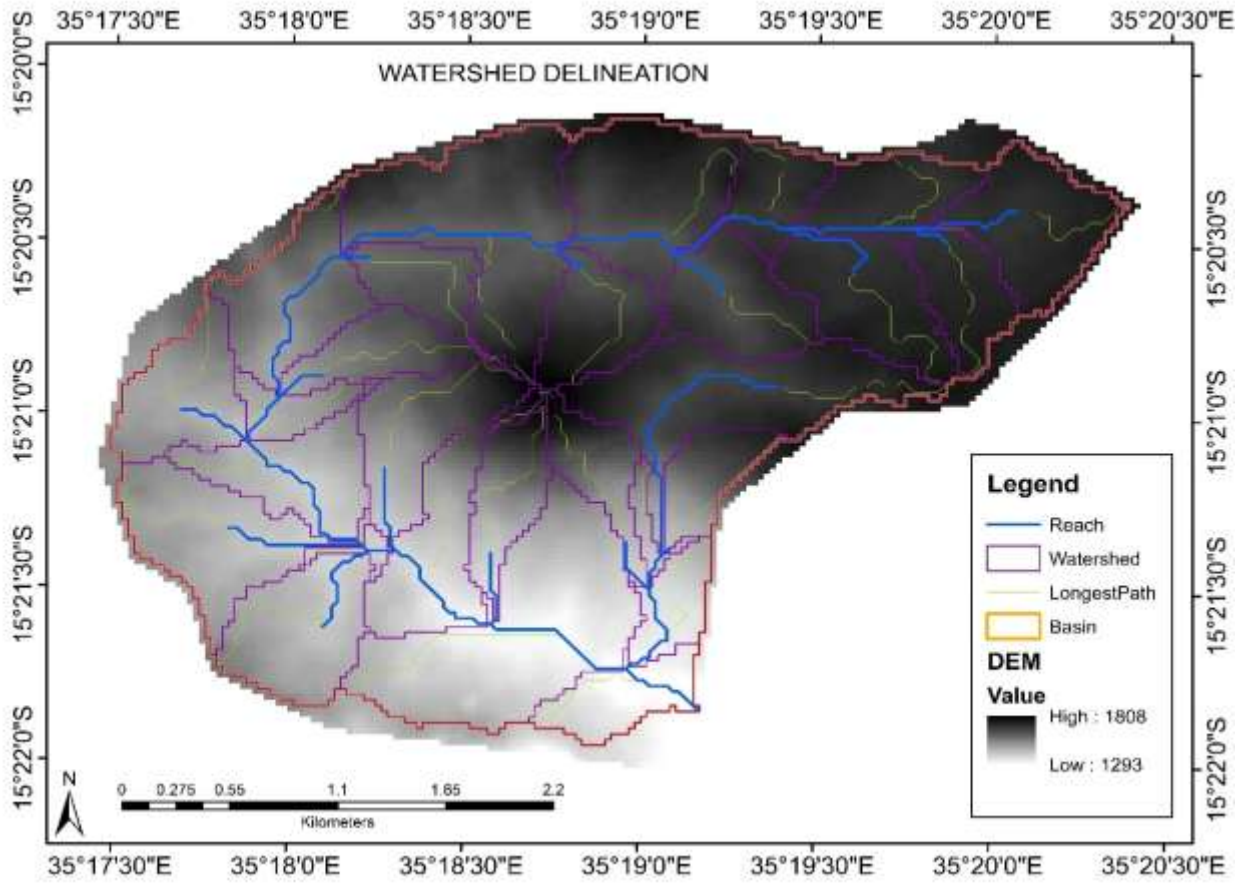

Figure 4: Mulunguzi Watershed delineation

3.4.3.2 HRU analysis

The model conducted an HRU analysis, which classified regions with similar parameters based on their soil type, land use, and slope. The SWAT model utilized the LULC images to analyze the hydrological responses of the watershed after classification. A lookup table was implemented to transform the classified images into a SWAT code-recognized database. The corresponding SWAT database values include 1=FRSE (Evergreen Forested Area), 154=FRST (Mixed Forest Area), 204=AGRL (Generic Agriculture), 219=WATR (Water bodies), and 225=BARR (Barren Land). For additional details, please see Appendix A1.

Figure 5 demonstrates the import of the soil map to account for soil properties within the watershed. Soil properties such as texture, organic carbon content, bulk density, hydraulic conductivity, and available water content play a crucial role in the runoff of the watershed. The FAO soil map developed for the Mulunguzi watershed only depicted one type of soil, I-Bc-c (Lithosols). The soil map was reclassified into the user-soil MWSWAT database using the lookup table in Appendix A2 and assigned a value of 644. Furthermore, the watershed was classified based on five slope classes: 0-10%, 10-15%, 15-20%, 20-30%, and >30%, as shown in Figure 6.

The comprehensive map was created by merging the LULC, soil, and slope classifications. Afterward, the HRU definition was applied to the sub-basin area using a 10% threshold for Land Use, 5% for Soil data, and 5% for Slope data. Then, elevation bands were automatically calculated, and HRUs were generated. The Mulunguzi watershed was divided into 30 sub-basins, resulting in 275 HRUs (Appendix B1).

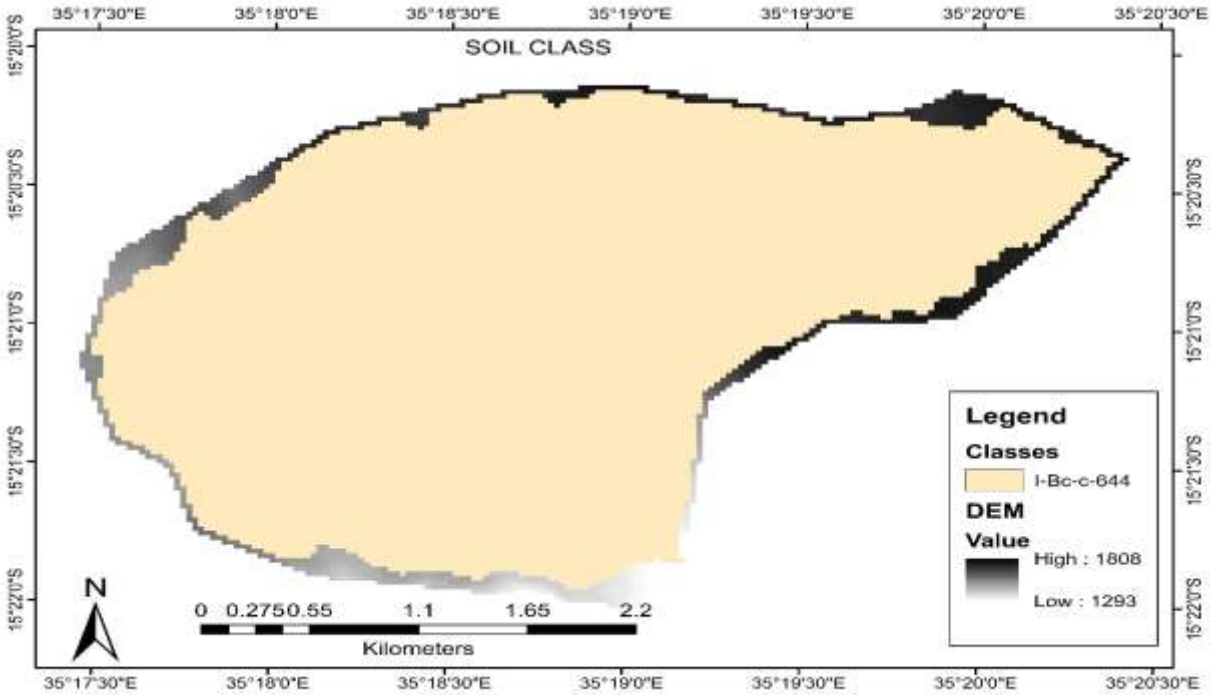

Figure 5: Soil Map depicting Lithosols

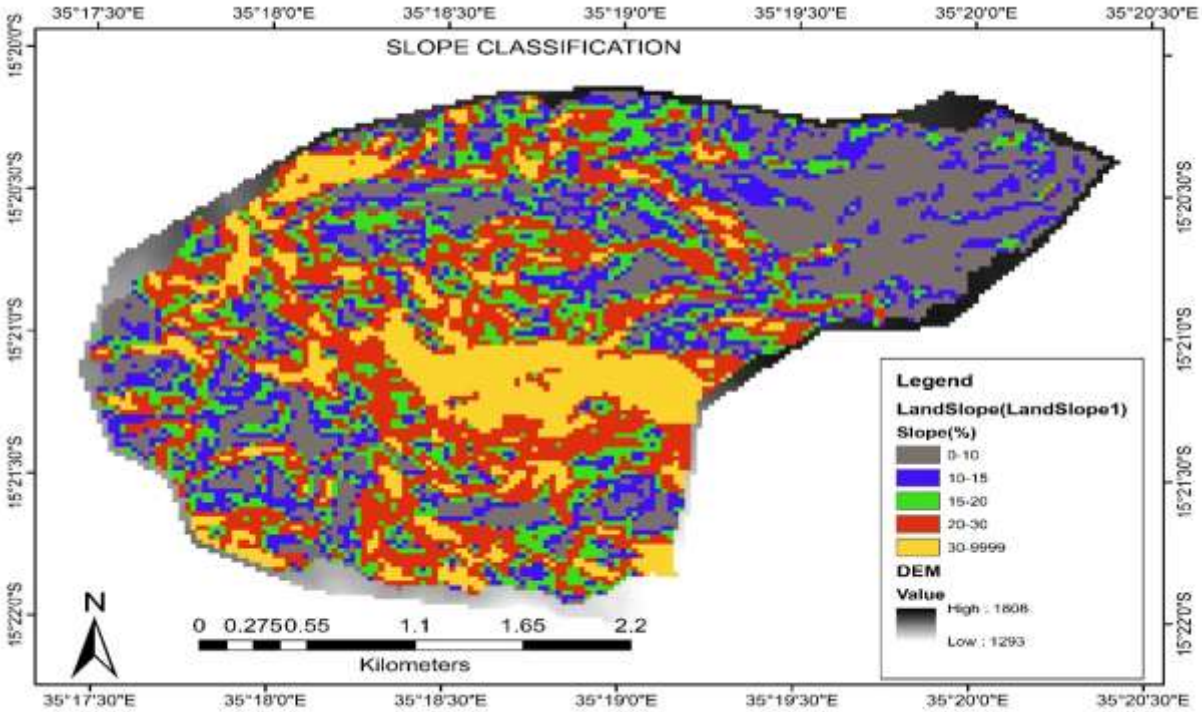

Figure 6: Slope Classification

3.4.3.3 Weather Data

A specific part of the model was dedicated to writing SWAT input tables. Section 3.6.2 describes updating the SWAT database with climate data from three stations. Daily rainfall, minimum, and maximum temperature data were imported through text files in Appendices C1 and C2. At the same time, the SWAT weather generator (WGEN) function was used to generate solar radiation, relative humidity, and wind speed data (Meins, 2013).

After completing all the necessary procedures, the SWAT model was prepared to run with 1990 as a warm-up period.

3.4.4 Sensitivity Analysis

Abbaspour et al. (2012) developed the SWAT-CUP tool, which was utilized to enhance the model's calibration and validation. The tool can determine the most sensitive parameters of a watershed, which play a critical role in ensuring successful model calibration and validation. The SUFI-2 algorithm introduced by Abbaspour & Johnson in 2004 is utilized in the SWAT-CUP package to aid in model calibration, validation, and sensitivity analysis. Like Woldesenbet et al. (2017), the parameters chosen for sensitivity analysis are displayed in Table 3. Two statistical indices were utilized to measure and assess sensitivity: the student's t-stat and the p-value. The t-stat measures a parameter's sensitivity, while the p-value evaluates the statistical significance of this sensitivity. These indices together offer a thorough comprehension of how each parameter affects the performance and output of the SWAT model.

Table 3. Selected parameters for sensitivity analysis

Parameter	Description	Min_value	Max_value
CN2	The initial Curve Number used to determine the amount of water that is converted to surface runoff	-0.2	0.2
SOL_BD	Determines the moist bulk density	0	1
GW_DELAY	The lag time between water exiting the soil profile and entering the shallow aquifer	30	450
ESCO	Configures the depth of the soil at which water can still evaporate from the soil	0	2
ALPHA_BF	Direct index of groundwater flow response to changes in recharge	0	1
CH_N2	Manning's roughness coefficient of the main river in a sub-basin	0	1
GWQMN	Groundwater flow to the reach is allowed only if the depth of water in the shallow aquifer is equal to or greater than GWqmn	-0.01	0.3
SURLAG	Controls the fraction of available water that will be allowed to enter a reach on a day	0	24
CANMX	The maximum amount of water that can be intercepted and stored in a fully developed canopy	0	100
GW_REVAP	Determines the ease with which water can transfer from the shallow aquifer to the soil profile	0	1
EPCO	Configures how much water can be taken up by plants from deeper soil layers	0	1
ALPHA_BF	Direct index of groundwater flow response to changes in recharge	0	1

3.4.5 Calibration and Validation

Calibration and validation are done to improve the accuracy of model predictions. The split-sample technique divided the observed flow data into two parts for calibration and validation. SUFI-2 algorithm was employed for calibration and validation using the SWAT-CUP 2012 software.

The calibration phase spanned from 1991 to 2005, with 1990 set as a warm-up year, while validation occurred from 2006 to 2020, relying on observed streamflow data. Statistical metrics were employed to evaluate the model performance according to the guidelines set by Moriasi et al. (2007). This involved calculating the NSE, RSR, and PBIAS. To be considered acceptable, the simulation of streamflow had to meet specific criteria: NSE greater than 0.5, RSR less than or equal to 0.70, and PBIAS within ±25%. In addition to these metrices, the Mean Absolute Error (MAE) was also employed to provide a direct measure of the model performance. MAE ranges between 0 and 1, with values closer to 0 indicating the model's best performance. Scatter plots and flow duration curves (FDC) were also utilized, like Nkhoma et al. (2021). All these methords, provided a holistic approach in model performance assessment.

The statistical indices were calculated using the equations listed below:

$$\text{NSE} = 1 - \left[\frac{\sum_{i=1}^{n}(Y_i^{obs} - Y_i^{sim})^2}{\sum_{i=1}^{n}(Y_i^{obs} - Y_i^{mean})^2}\right] \quad \text{(i)}$$

$$\text{the RSR} = \frac{RSME}{STDEV_{obs}} = \frac{\left[\sqrt{\sum_{i=1}^{n}(Y_i^{obs} - Y_i^{sim})^2}\right]}{\left[\sqrt{\sum_{i=1}^{n}(Y_i^{obs} - Y_i^{mean})^2}\right]} \quad \text{(ii)}$$

$$\text{PBIAS} = \left[\frac{\sum_{i=1}^{n}(Y_i^{obs} - Y_i^{sim})*(100)}{\sum_{i=1}^{n}(Y_i^{obs})}\right] \quad \text{(iii)}$$

$$\text{MAE} = \frac{1}{n}\sum_{i=1}^{n}|Y_i^{obs} - Y_i^{sim}| \quad \text{(iv)}$$

In these equations, Y_i^{obs} is the ith observation for the constituent being evaluated, Y_i^{sim} is the ith simulated value for the constituent being evaluated, Y^{mean} is the mean of observed data for the constituent being evaluated, and n is the total number of observations.

3.4.6 Establishing Scenarios to Quantify the Impacts of Land Use and Climate Changes

The study employed the One-Factor-At-A-Time (OFAT) approach to quantify the impacts of LULC alterations and CC. The methodology used in this research aligns with the approaches used by Tan et al. (2015) and Nkhoma et al. (2021) in their respective studies. The study defined several scenarios (Sc) to analyze different aspects.

1. Baseline: This scenario employed 1990 LULC and climate data from 1990 to 1997.
2. Land Use Change: These scenarios involved the LULC data of 2000 and 2021 but kept the climate data consistent with the baseline scenario. The scenarios isolated the impact of LULC changes.
3. Climate Change: These scenarios kept the LULC data consistent with the baseline (1990 map) but used climate data progressively from 1990-1997, 1998-2008, and 2009-2020. The scenario was used to evaluate the effects of climate change.
4. Combined LULC and CC: The scenario employed the LULC Map for 2000 and 2021, with corresponding years of climate data.

The student's t-test was employed to evaluate the differences in discharge under the different scenarios;

$$t=\frac{\overline{X}_1-\overline{X}_2}{\sqrt{\frac{{S_1}^2}{n_1}+\frac{{S_2}^2}{n_2}}} \quad \text{.....(iv)}$$

Where: $\overline{X}_1$ and $\overline{X}_2$ are the mean discharges under the two different scenarios; S_1 and S_2 are the standard deviations (square roots of the variances) of the discharges under the two scenarios; n_1 and n_2 are the numbers of data points (number of simulated years) for the two scenarios. The null hypothesis is accepted at a 95% confidence level if $|t|<1.96$ and rejected otherwise (Nkhoma et al., 2021).

CHAPTER FOUR

RESULTS AND DISCUSSIONS

4.1 Changes in Land Use and Land Cover from 1990 to 2020

Table 4, Figures 7 and 8 indicate that the Mulunguzi catchment has experienced a significant reduction in forest land, which decreased from 46.97% in 1990 to 23.93% in 2020. This represents a 23.04% reduction in heavily forested areas. The primary contributing factor is deforestation caused by illegally harvesting pine trees for timber processing. According to the Zomba Social and Economic Profile (2017-2020), a minimum of 100 timber trees are illegally harvested every month, driven by the high demand for timber in Zomba City. The profile further reported an encroachment in the forest land for agricultural production by the surrounding communities. This explains the increase in agricultural and bare land by 4.7% and 11.8%, respectively, between 1990 and 2020. During the same period, grassland areas increased from 31.89% to 40.55%. These findings are consistent with Kambombe (2018) observation that an increase in grassland area leads to decreased forest land in the MRB.

Table 4 Area and percentage of LULC classes in the MRB

Land Use Classes	**1990 Area(km^2)**	**(%)**	**2000 Area(km^2)**	**(%)**	**2020 Area(km^2)**	**(%)**	**Change (km^2) 1990-2020**	**Change (%) 1990-2020**
Forest Land	11.96	46.97	10.19	40.04	6.09	23.93	-5.87	-23.04
Grass Land	8.12	31.89	10.78	42.36	10.32	40.55	2.2	8.66
Agricultural Land	2.67	10.50	3.55	13.95	3.87	15.21	12.54	4.71
Water Body	0.71	2.80	0.13	0.51	0.17	0.65	-0.06	-2.15
Bare Land	1.99	7.84	0.80	3.14	5.00	19.66	17.67	11.82
Total	25.45	100	25.45	100	25.45	100		

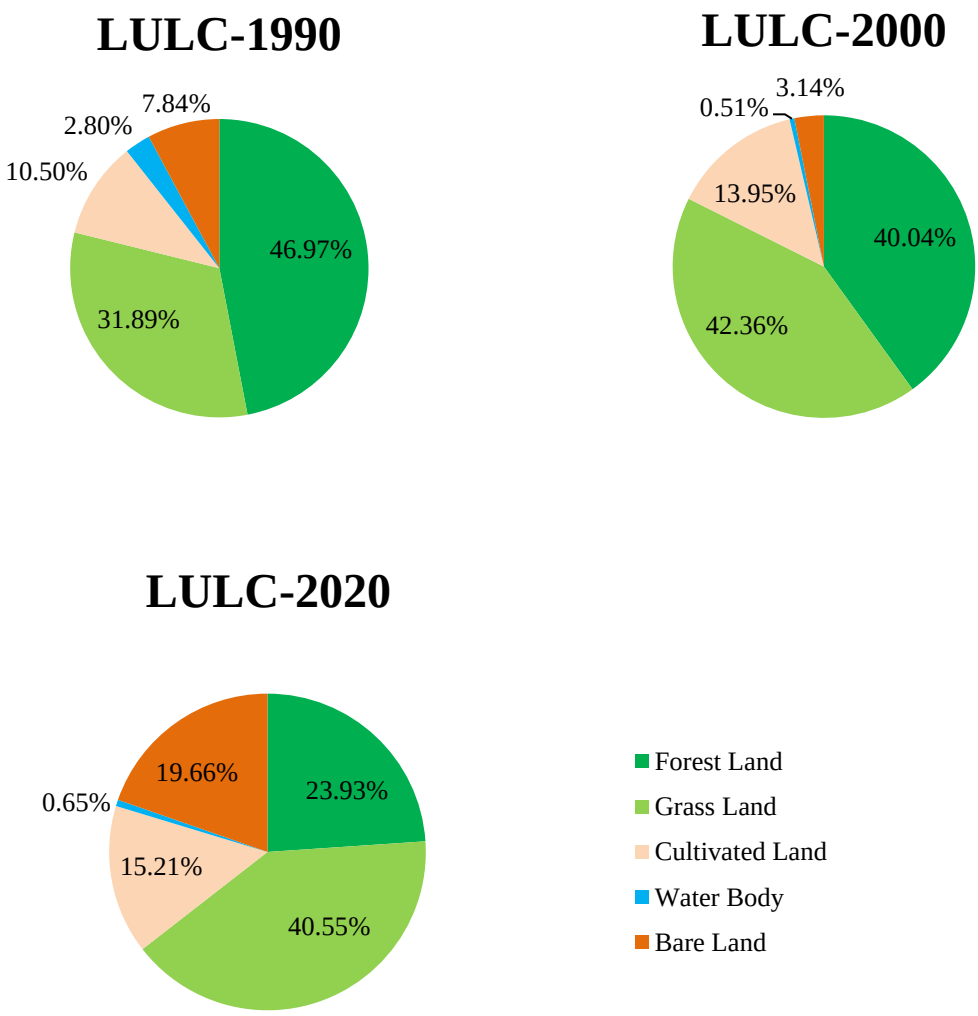

Figure 7: Time Series Pie Charts for LULC

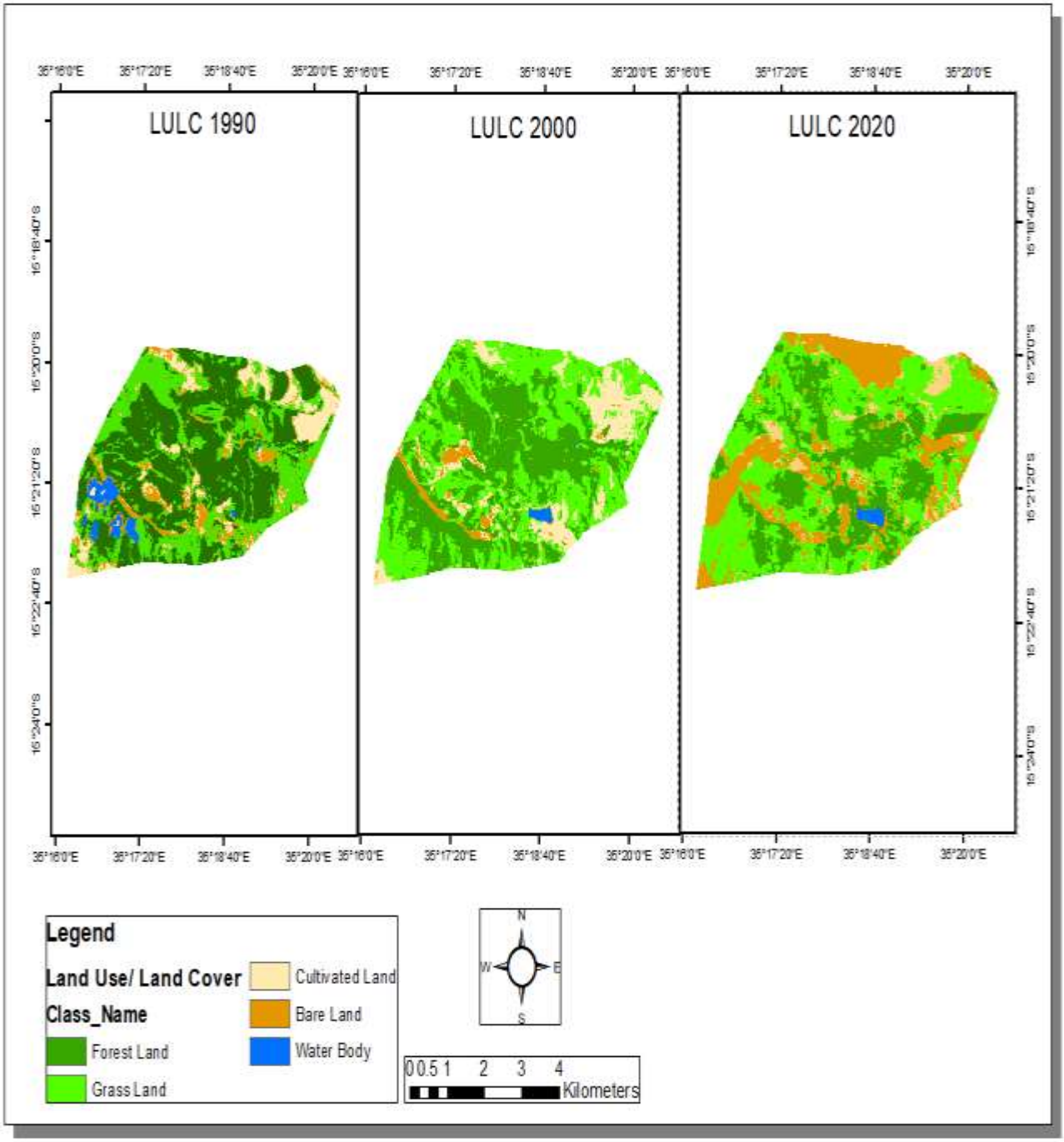

Figure 8: Land Use and Land Cover Change Maps

4.2 Temporal Trends of the Hydroclimatology

Hydrological components of the MRB are affected by climatic inputs, among other factors. The impacts of climatic variability were understood separately and combined with other inputs to evaluate the causes of change in the flows of the Mulunguzi River. Man-Kendall test was used for trend analysis, and Sen's slope was employed to estimate the magnitudes of these trends.

4.2.1 Analysis of Temperature Trends

The analysis of Temperature data between 1990 and 2020 showed that the mean annual temperature in the basin was 22.75°C. The mean maximum and minimum temperatures were 24.5°C and 21°C, respectively. The results agree with the research conducted by Ngongondo et al. (2015), which stated that Malawi's average annual temperature was 22.6°C between 1971 and 2000. Table 5 shows that there has been a rise in the average monthly temperatures, increasing by 0.004°C every month. In figure 9 there was a rise in average annual temperature at 0.041°C per year, this trend did not reach statistical significance at the 95% confidence level. In comparison, Ngongondo et al. (2015) identified a statistically significant annual temperature increase of 0.03°C per year in Malawi from 1971 to 2000, slightly lower than the observed trend in the MRB. Table 5 and figure 11 show a statistically significant increase at α=0.05 in monthly and yearly minimum temperatures (Tmin), with rates of 0.01°C per month and 0.112°C per year, respectively. On the contrary, monthly and yearly maximum temperatures have decreased, with a reduction of 0.002°C per month and 0.033°C per year, as illustrated in Figure 10. However, the decreasing trend in maximum temperatures did not achieve statistical significance at the α=0.05 level.

Table 5 Mann Kendal and Sen's Slope Test results.

	Monthly			Annually		
	P-value	**Sen's Slope**	**Tau**	**P-value**	**Sen's Slope**	**Tau**
Tmax	0.002	-0.002	-0.107	0.221	-0.033	-0.157
Tmin	**1.75E-06**	**0.010**	**0.354**	**0.005**	**0.112**	**0.359**
Mean	2.38e07	0.004	0.178	0.103	0.041	0.209

Data in Figure 9 shows that there has been a stable increase in the Areal mean annual temperature since 1990, with a rise of 1.2°C by 2020. The mean annual temperature in 2002 was 20.4°C, the lowest on record. This was due to the lowest minimum temperatures recorded between May and August, reaching up to 15°C. Figures 10 and 11 present a decline in the Areal mean maximum temperature and a rise in the mean minimum temperature during the same timeframe. The rise in mean annual temperature is believed to be a consequence of human-caused climate change, as noted by Ngongondo et al. (2015). The 2023 IPCC report asserts that the global surface temperature has risen by 1.1°C due to global warming (Calvin et al., 2023). Wodaje et al. (2021) and Tan et al. (2015) have also identified comparable patterns in Ethiopia and Malaysia, respectively.

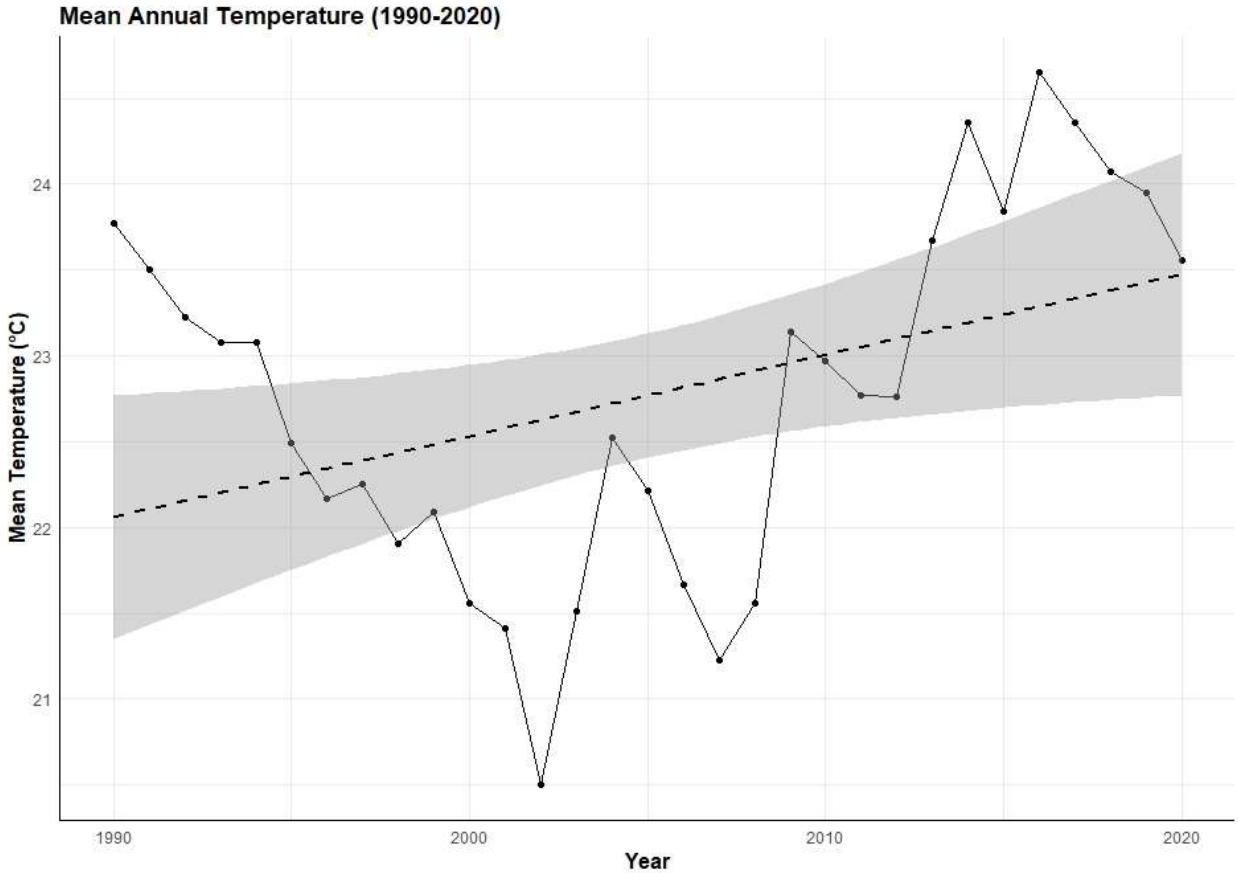

Figure 9: Mean Annual Temperature from 1990-2020

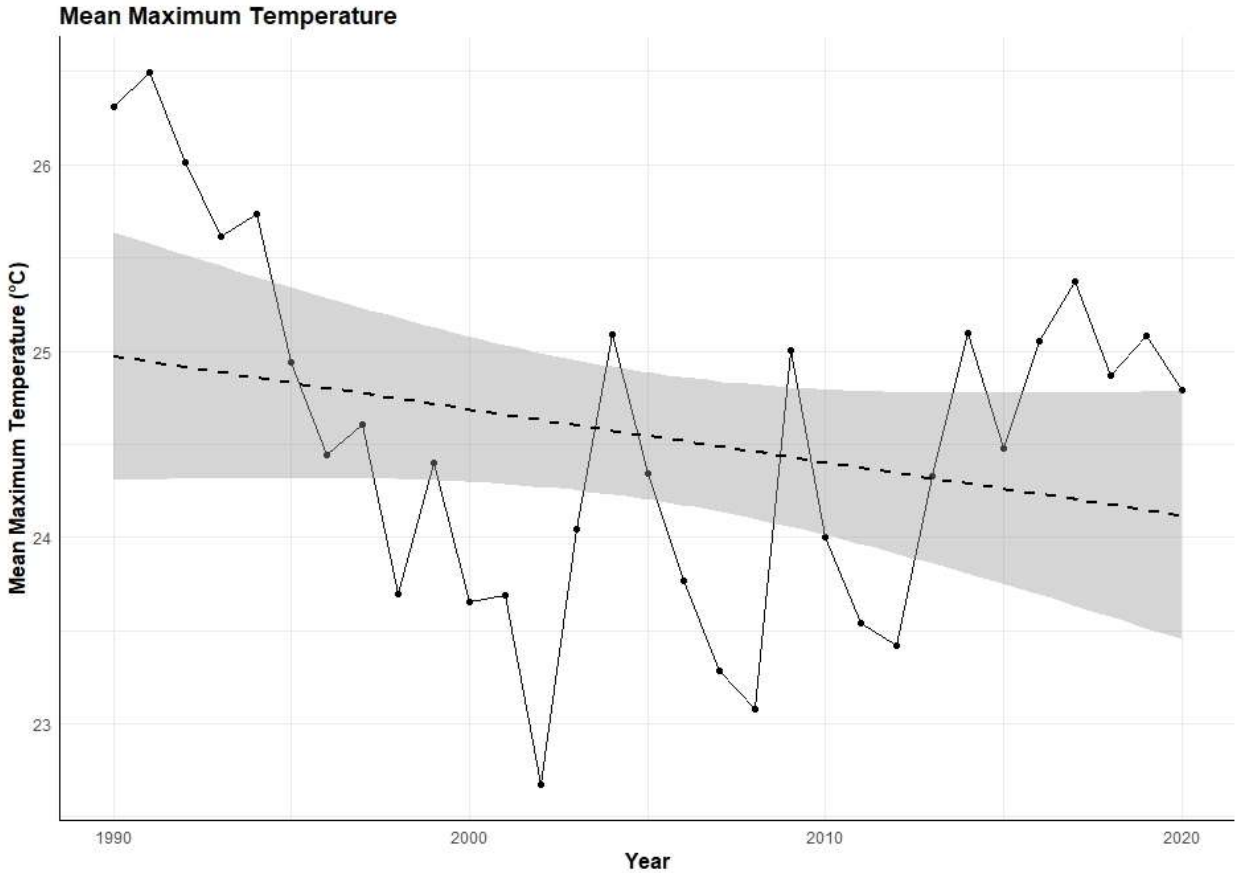

Figure 10: Linear Trend Mean Annual Maximum Temperature

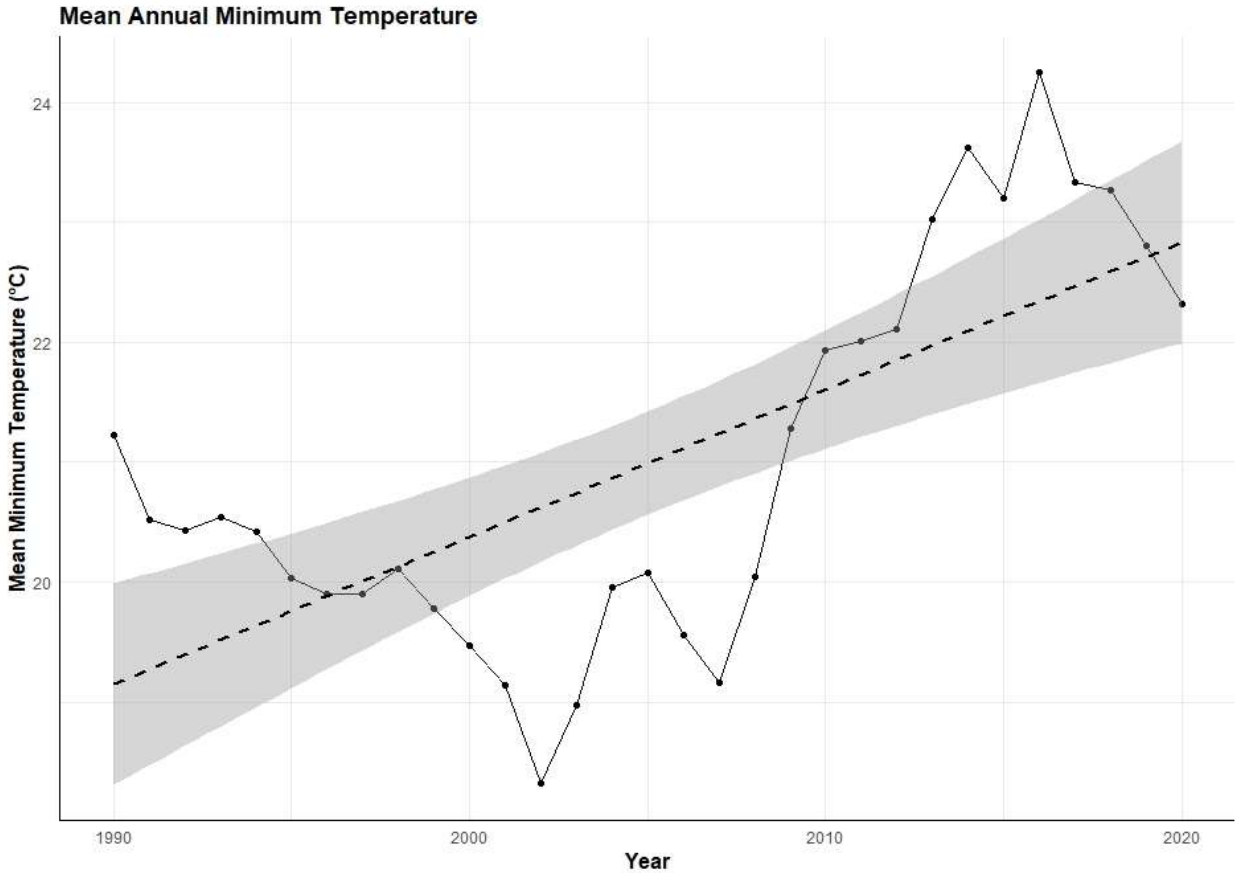

Figure 11: Linear Trend Mean Annual Minimum Temperature

4.2.2 Rainfall

The statistical analysis reveals that the mean annual rainfall in the region was 990 mm between 1990 and 2020, with a coefficient of variation of 26.27%. The wet and dry seasons witnessed an average annual rainfall of 1055.17 mm and 143.14mm, respectively. These findings align with those of Ngongondo et al. (2011), which reported an average annual rainfall of 1083 mm across the country with a coefficient of variation of 26%.

4.2.2.1 Trends in Rainfall

The results of the MK test in Table 6 exhibit a rise in precipitation for most months except August, September, and November. Rainfall significantly increased in May and July, while it significantly decreased in August. This implies that there was a noticeable reduction in rainfall during August throughout the study period. The annual, wet, and dry timescales had increasing trends but were not statistically significant at α=0.05. In Figure 12, rainfall has increased to 5.81mm per year from 1990 to 2020. Mbano et al. (2009) reported a decreasing trend at monthly, annual, and seasonal scales between 1954 and 1993, which contrasts with the results found in this study. Differences in study periods and the impact of climate change over time, as shown in Figure 13 during the decadal trend analysis, can account for the observed variations.

In Figure 13, an analysis was conducted to understand the trend of rainfall among the three decades: 1990-1999 (1990s), 2000-2009 (2000s), and 2010-2020 (2010s). The statistical findings showed that rainfall trends in all decades were insignificant at α=0.05. The 1990s and 2010s experienced an increasing trend at 44mm and 18 mm per year, respectively. However, there was a downward trend in the 2000s at 10 mm per year. Chauluka et al. (2021) noted a comparable observation while examining rainfall and streamflow trends in the Thuchila River in Southern Malawi. They found that from 1985 to 2015, there was a decreasing trend, but it was not statistically significant. The variability in rainfall over these decades is attributed to the impacts of climate change over time (Tan et al., 2015).

Over the last three decades, analyzing rainfall amounts has revealed a fascinating insight into how rainfall is distributed over time. Although there was a downward trend in the 2000s, the cumulative rainfall was higher than in the 1990s. As shown in Figure 14, the 2010s had the highest cumulative rainfall at 9529 mm, followed by the 2000s with 9410 mm, and the lowest was the 1990s with

9382 mm. The variations in rainfall across the decades are attributed to extreme rainfall events in specific years. As shown in Figure 15, the highest peaks were observed in the 2000s and 2010s over the past three decades, while the 1990s registered the lowest amount of rainfall, especially between 1990 and 1995. Between 1991 and 1994, Southern Africa underwent a drought period due to the cycles of El Nino and Southern Oscillation (ENSO) and La Nina, as per a study by Richard et al. (2001). A comparable outcome was observed by Ngongondo (2005) while examining the long-term variability of rainfall in the Mulunguzi catchment.

Table 6 MK results and Sen's Slope results

Period	Z-Value	P-Value	Sen's Slope	Trend	95% Confidence
January	1.36	0.17	2.41	Increasing	No
February	1.43	0.15	2.85	Increasing	No
March	1.02	0.31	2.03	Increasing	No
April	0.51	0.61	0.43	Increasing	No
May	**2.52**	**0.01**	**0.67**	**Increasing**	**Yes**
June	1.91	0.05	0.19	Increasing	No
July	**2.75**	**0.01**	**0.36**	**Increasing**	**Yes**
August	**-2.41**	**0.016**	**-0.14**	**Decreasing**	**Yes**
September	-0.34	0.73	-0.02	Decreasing	No
October	0.78	0.43	0.13	Increasing	No
November	-0.41	0.68	-0.37	Decreasing	No
December	0.17	0.87	0.17	Increasing	No
Wet Season	1.16	0.25	6.49	Increasing	No
Dry Season	1.16	0.25	1.27	Increasing	No
Annual	1.02	0.31	5.81	Increasing	No

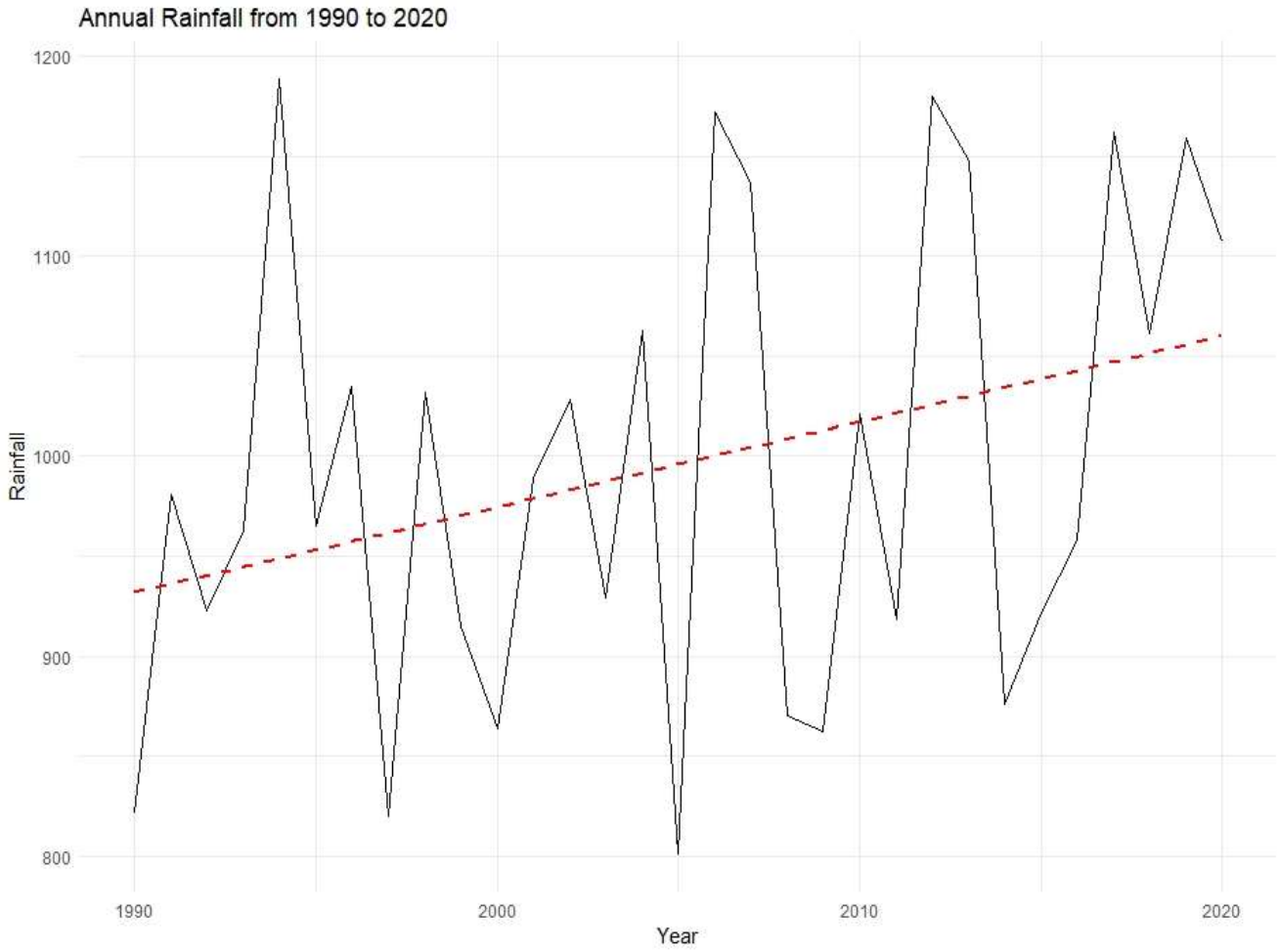

Figure 12: Annual Rainfall Trend from 1990 to 2020

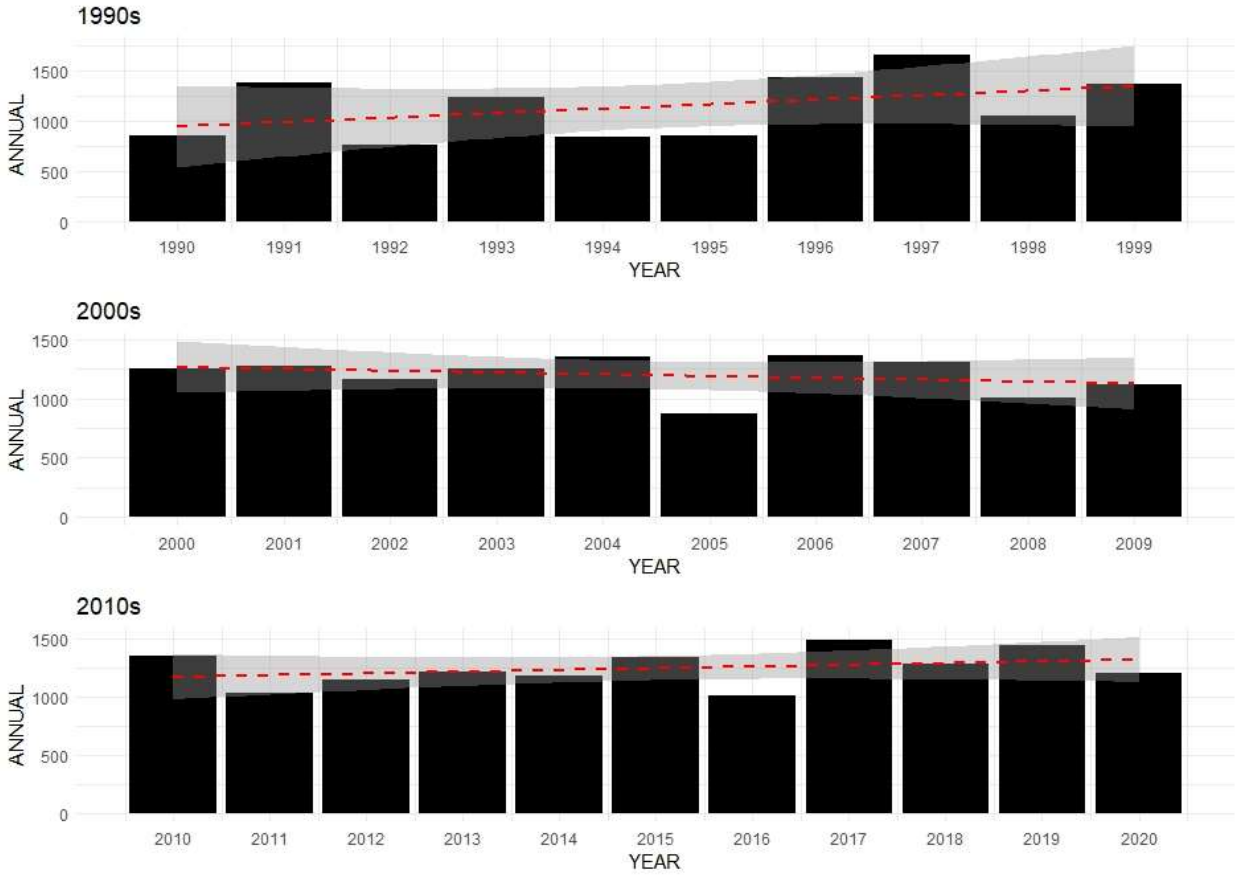

Figure 13: Trend Analysis within the Three Decades

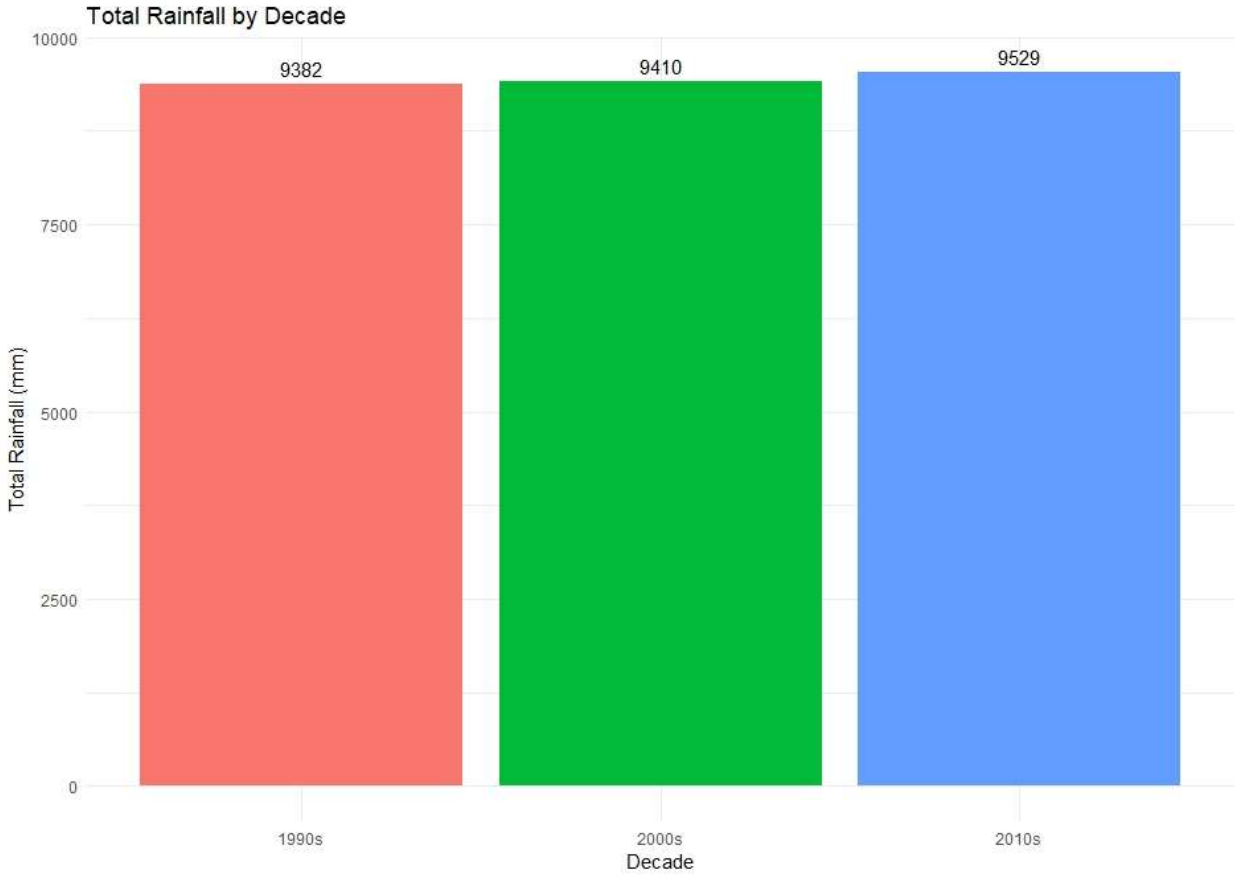

Figure 14: Total rainfall in the three decades

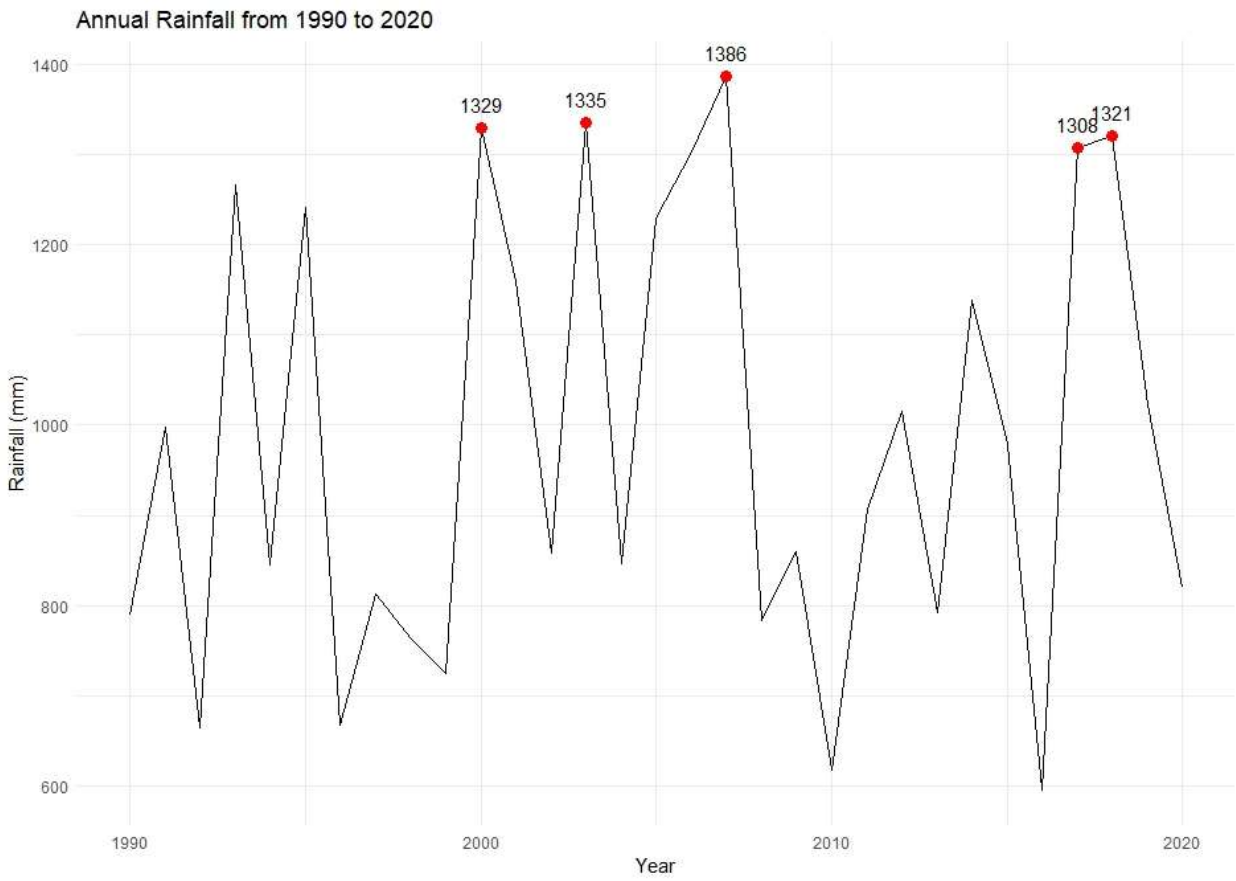

Figure 15: Annual Rainfall with Peak Years

4.2.3 River Discharge Trends

The Mulunguzi River had an average streamflow of 0.3 m^3/s from 1990 to 2020, with a coefficient of variation of 30.1%. During the wet season, the streamflow was 0.4 m^3/s, while during the dry season, it was 0.2 m^3/s. In comparison, Ngongondo (2005) reported that from 1953 to 1998, the mean annual flow was 0.5 m^3/s with a coefficient of variation of 38%. The difference in mean flow between the two studies is not significant. It is attributed to the difference in study periods.

4.2.3.1 Trends in Streamflow

From 1990 to 2020, the Mulunguzi River experienced a dominant decreasing trend in monthly and annual flows. According to Sen's Slope results, the flow is decreasing in Figures 16 and 17 with a magnitude of 0.0000067 m^3/s per month and 0.0012 m^3/s per year, respectively. Additionally, the MK statistics results for the monthly series showed a statistically significant trend at $\alpha = 0.05$ with a p-value of 0.041. The Tau value -0.07 suggests a weak downward trend in the monthly data. On the other hand, the annual series did not show a statistically significant trend at $\alpha = 0.05$, with a p-value of 0.1489. Its Tau value of -0.18 indicated a weak decreasing trend in the flow data in the annual series.

In Figure 18, a comparison was made between rainfall and stream flow data from 1990 to 2020. Usually, we expect to see a direct correlation between rainfall and stream flow over time. However, despite consistent rainfall, there has been a general decrease in stream flow. This suggests that factors beyond rainfall, such as alterations in LULC, may impact the MRB's stream flow. Similar conclusions were reached by Nyatuame et al. (2020), who found that an increase in rainfall alone does not necessarily lead to increased runoff. The study found that LULC plays a crucial role in determining the water yield of watersheds.

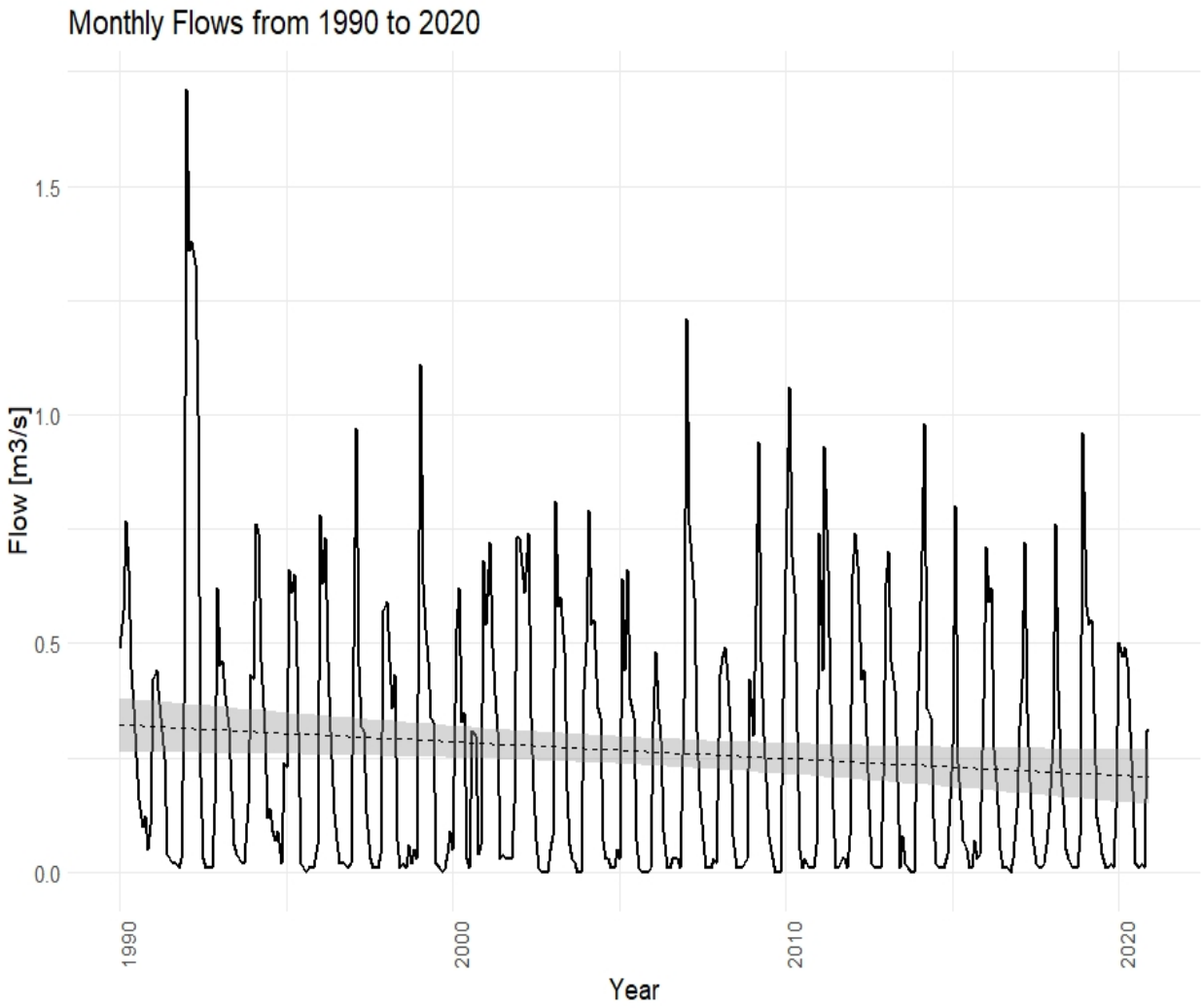

Figure 16: Trend of Streamflow at Monthly Series

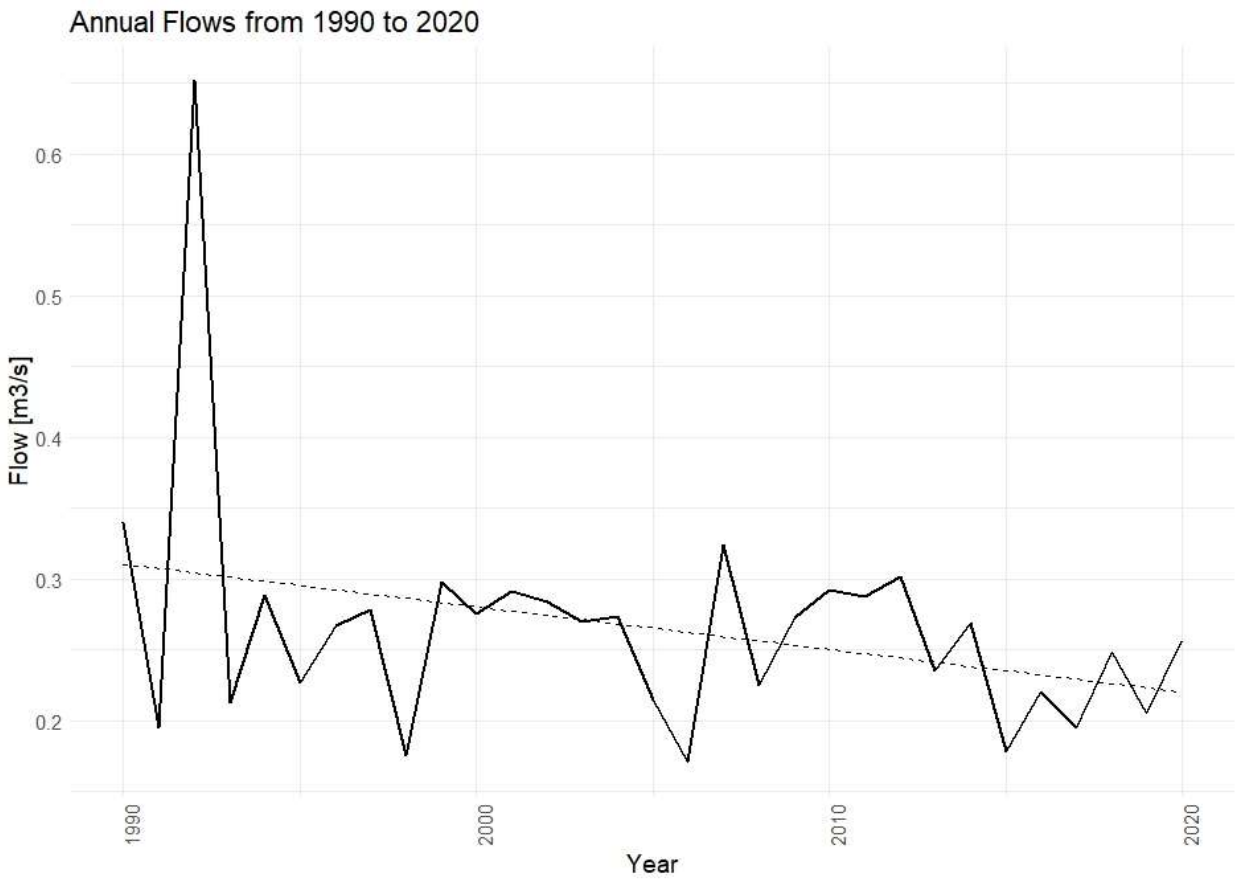

Figure 17: Trend of Streamflow at Annual series

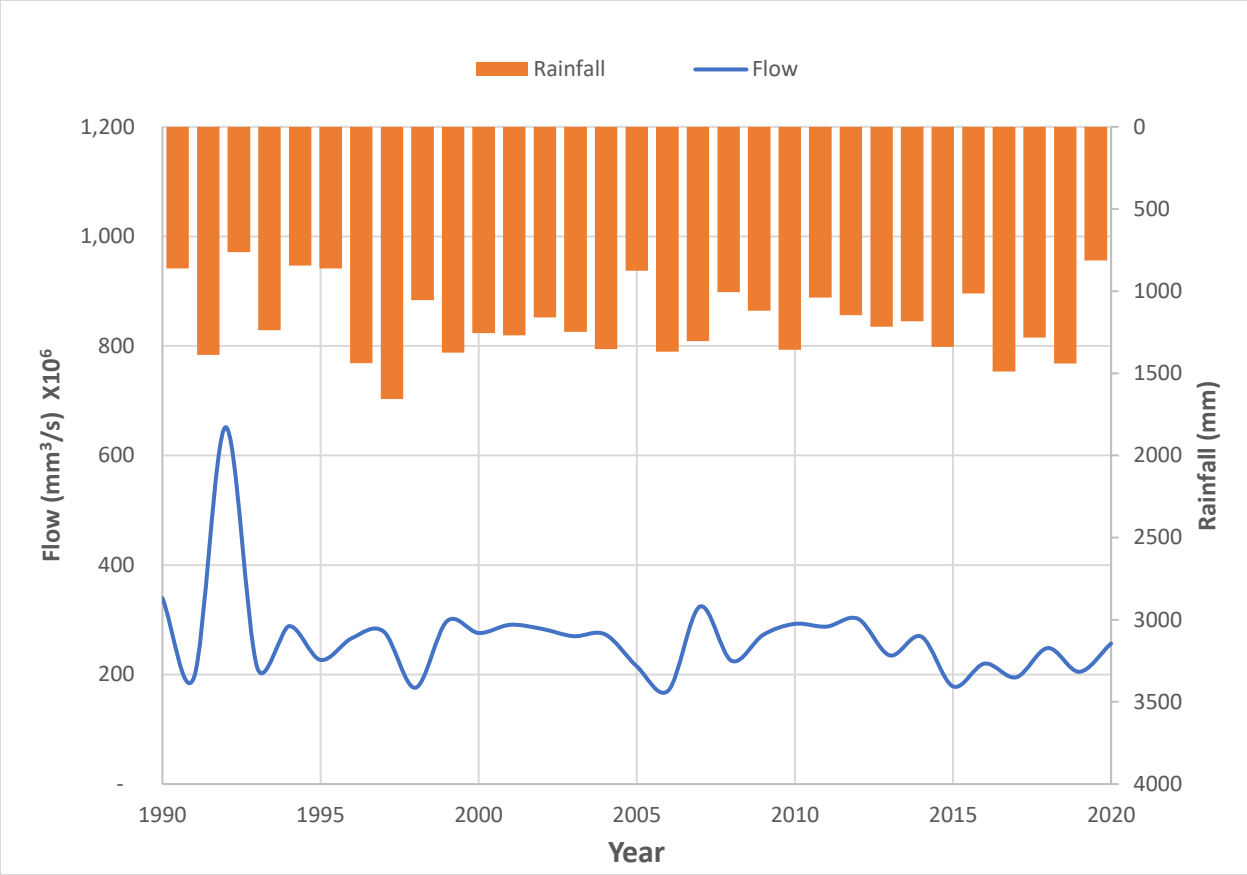

Figure 18: Annual rainfall and stream flow for Mulunguzi watershed

4.3 The SWAT Model.

4.3.1 Sensitivity analysis

The SUFI2 algorithm is widely utilized for global sensitivity analysis and calibration in the SWAT model. Figure 19 displays the evaluation of model parameters, which were assessed using their P-values and T-statistics. A higher absolute T-stat value indicates a more significant influence of a parameter on the model's output, while a small P-value (≤ 0.05) shows statistical significance. The parameters were ranked based on their sensitivity, from the most to the least sensitive, and presented in Table 7. These ranked parameters were then used in various scenarios with their calibrated values.

Six of the twelve parameters evaluated in the global sensitivity analysis were particularly sensitive for this study. These parameters are CN2, which represents the runoff curve number; SOL_BD, which stands for moist bulk density; GW_DELAY, which represents the groundwater delay; ESCO, which is the soil evaporation compensation factor; ALPHA_BF, which stands for the base flow alpha factor; and CH_N2, which represents Manning's value. The remaining parameters that were evaluated include GWQMN, which is the threshold water depth in the shallow aquifer for flow; SURLAG, which represents the surface runoff lag coefficient; CANMX, which is the maximum canopy storage; GW_REVAP, which is the groundwater revamp coefficient; EPCO, which stands for plant uptake compensation factor, and ALPHA_BF, which represents the base flow factor.

Table 7 Sensitivity Analysis

Parameter Name	t-Stat	p-value	Rank of Sensitivity	Fitted Value	Min_value	Max_value
CN2	-21.8629	0	1	-0.14	-0.2	0.2
SOL_BD	-18.1533	0	2	0.11	0	1
GW_DELAY	-16.21	0	3	209.90	30	450
ESCO	2.2501	0.0252	4	1.06	0	2
ALPHA_BF	1.7315	0.0844	5	0.20	0	1
CH_N2	-1.3132	0.1901	6	0.39	0	1
GWQMN	1.255	0.2105	7	0.14	-0.01	0.3
SURLAG	-0.838	0.4027	8	17.48	0	24
CANMX	0.7072	0.4799	9	56.17	0	100
GW_REVAP	-0.5444	0.5666	10	0.73	0	1
EPCO	0.35315	0.7242	11	0.42	0	1
ALPHA_BF	0.1395	0.8891	12	0.31	0	1

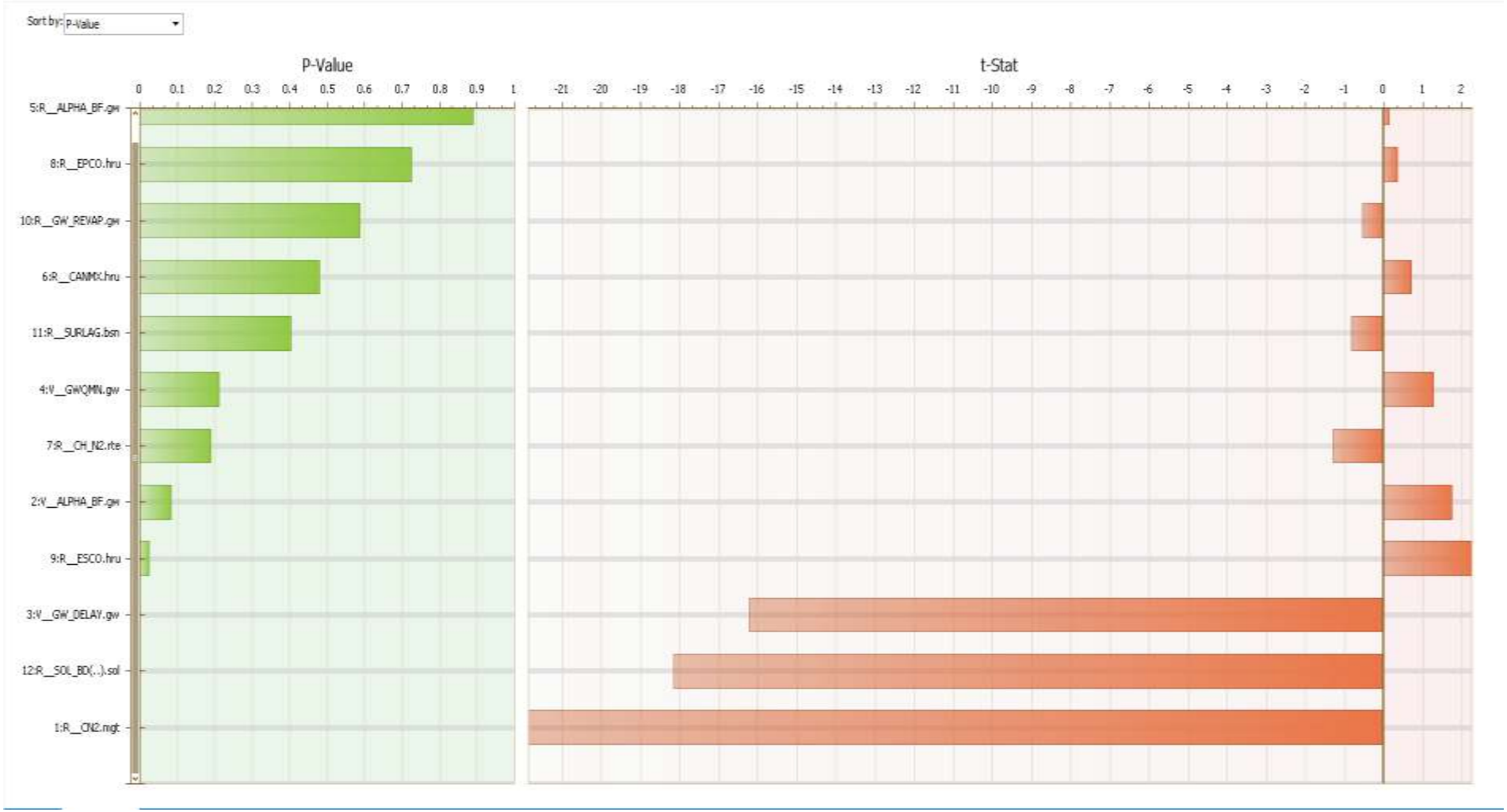

Figure 19: Global Sensitivity Analysis

4.3.2 Calibration and Validation of the SWAT model

Table 8 provides an overview of the model's performance. Using Moriasi et al. (2007) evaluation criteria, the model demonstrated adequate performance for NSE (0.54 to 0.65), satisfactory performance for PBIAS (<20%), and satisfactory performance for RSR (0.60 < RSR < 0.70) during the calibration phase. In the validation phase, the model exhibited excellent performance for NSE (>0.65), excellent performance for PBIAS (<10%), and excellent performance for RSR (0.00 < RSR < 0.50). The MAE of 0.06 and 0.11 in the validation and calibration phase, respectively, demonstrate the model's better performance during validation than during calibration. For example, the NSE value was higher during the validation period than in the calibration period, resulting from temporal variability and overall quality data in the validation than the calibration period, Gashaw et al. (2018) made similar observations. The statistics analysis indicates that the model is acceptable despite possibly overestimating and underestimating flows in the calibration and validation stages. These results agree with Nkhoma et al. (2021) in the Wankurumadzi Basin, Malawi, and Tan et al. (2015) in the Johor River Basin, Malaysia. Therefore, the SWAT model is appropriate for application in the MRB.

The simulated and observed flows for the Mulunguzi River are shown in Figures 20 and 21, respectively, covering the calibration period from 1991 to 2005 and the validation period from 2006 to 2020. The findings suggest that the simulated and observed flows are in good agreement. The model had some overestimations and underestimations during specific peak periods. However, the peak values of the simulation were generally in close agreement with those of the observation in the validation period. Figures 22 and 23 show that the model accurately simulated the actual flows more during the validation stage than in the calibration stage. In the calibration stage, the simulated flow did not closely follow the observed flows, even though the patterns were similar. The model both overestimated and underestimated peak and low flows in the calibration stage more than the validation stage. Figures 24 and 25 also demonstrate that the scatter plots are closer to the line of best fit in the validation stage than in the calibration stage. Despite this, the model showed adequate performance with an NSE value of greater than 0.54. The highest mean monthly discharge in the calibration phase was 0.9 m^3 in January, while that of the validation phase was 1.04 m^3 in February. The flow duration curve (FDC) shown in Figure 26 confirms the hydrological

model's accuracy, especially in its simulation of high-flow periods. The model's discharges closely matched the observed data for less than 20% probabilities, indicating a good representation of peak flow conditions. However, the model has limitations in the low-flow domain, specifically in underestimating the magnitude of base flow. This suggests potential errors in the model's parameters or structure regarding groundwater contributions or catchment storage dynamics. Additionally, the model's representation of intermediate to low-flow periods, ranging from 50% to 90% of probabilities, deviates from the observed data due to the model's sensitivity to hydrological processes governing flow persistence (Westerberg et al., 2011).

Table 8 Summary Statistics

Period	NSE	PBIAS	R^2	RSR	MAE
Calibration (1991-2005)	0.59	15.9	0.62	0.64	0.11
Validation (2006-2020)	0.83	4.0	0.84	0.41	0.06

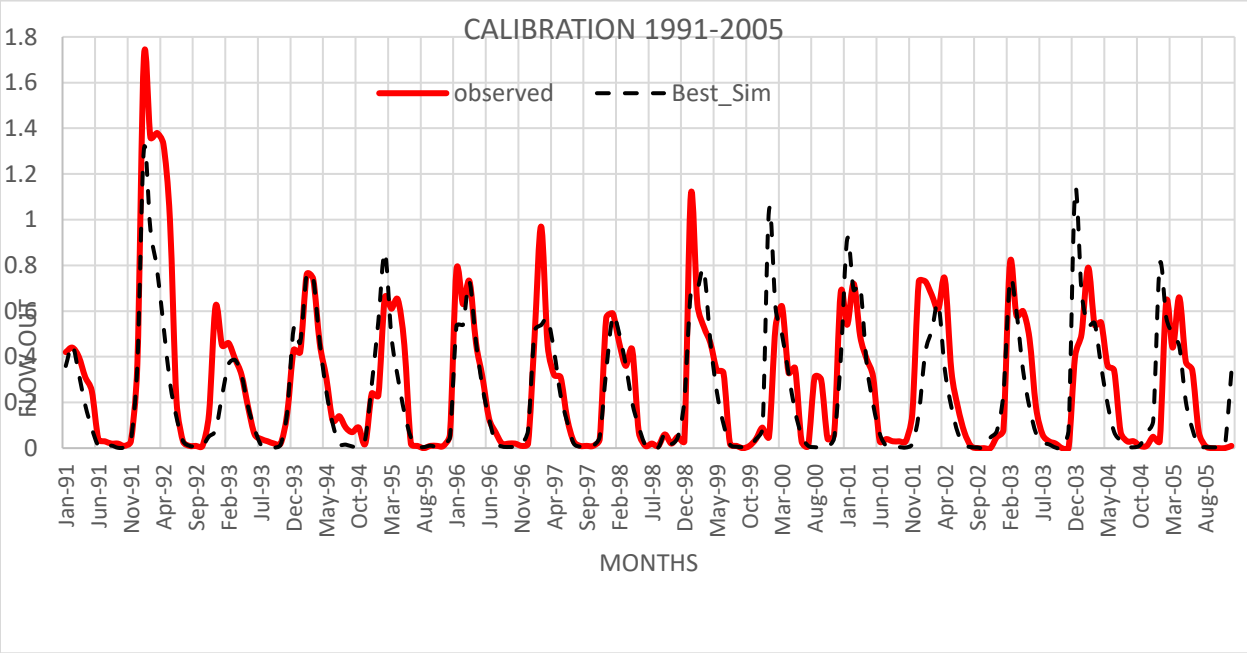

Figure 20: Observed and simulated flows during SWAT calibration.

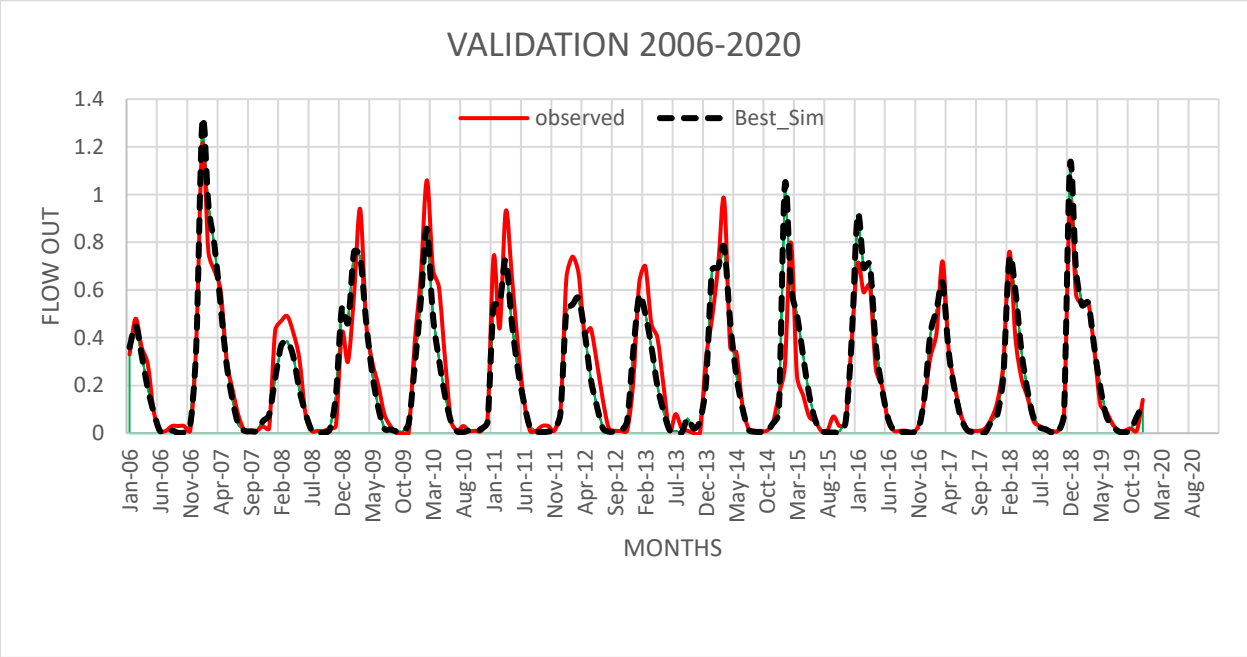

Figure 21: Observed and simulated flows during SWAT validation.

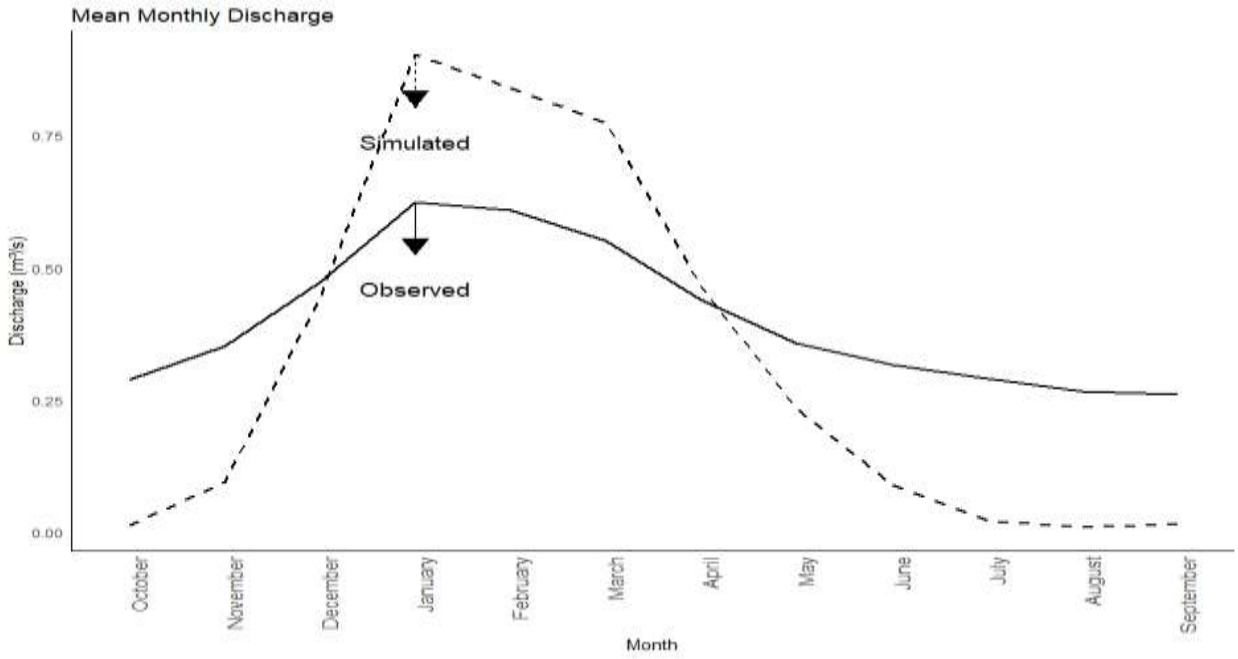

Figure 22: Mean monthly discharge during the calibration phase

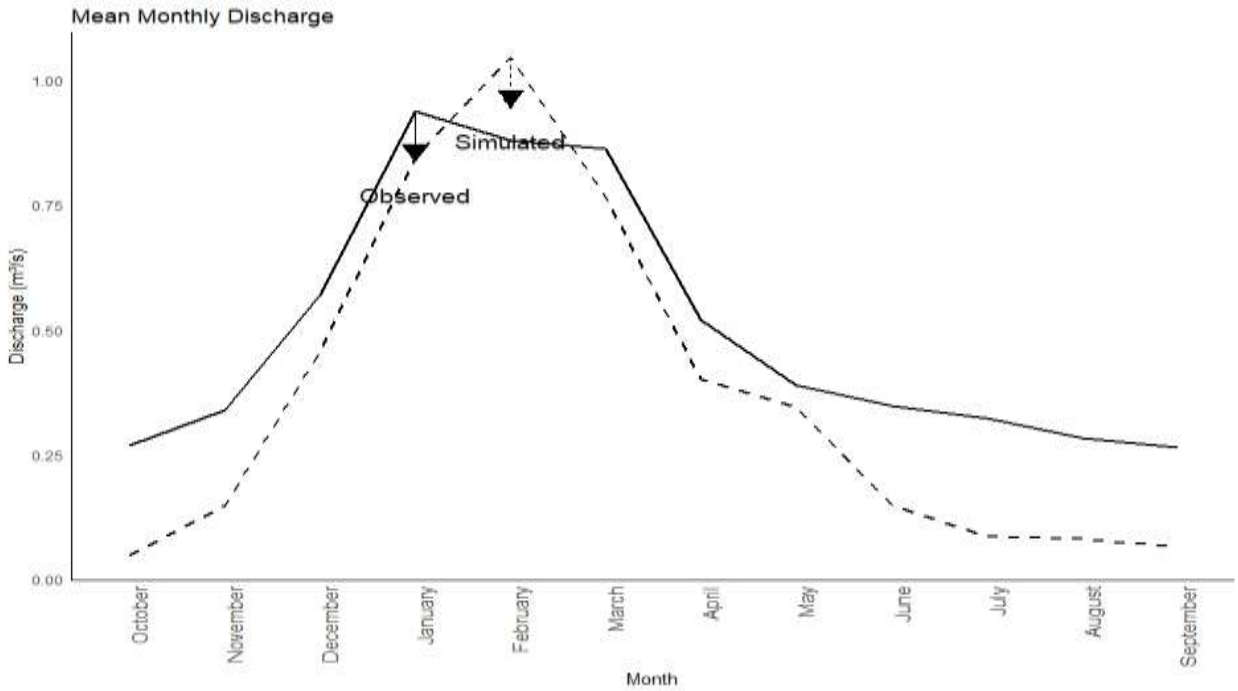

Figure 23: Mean monthly discharge during the validation stage.

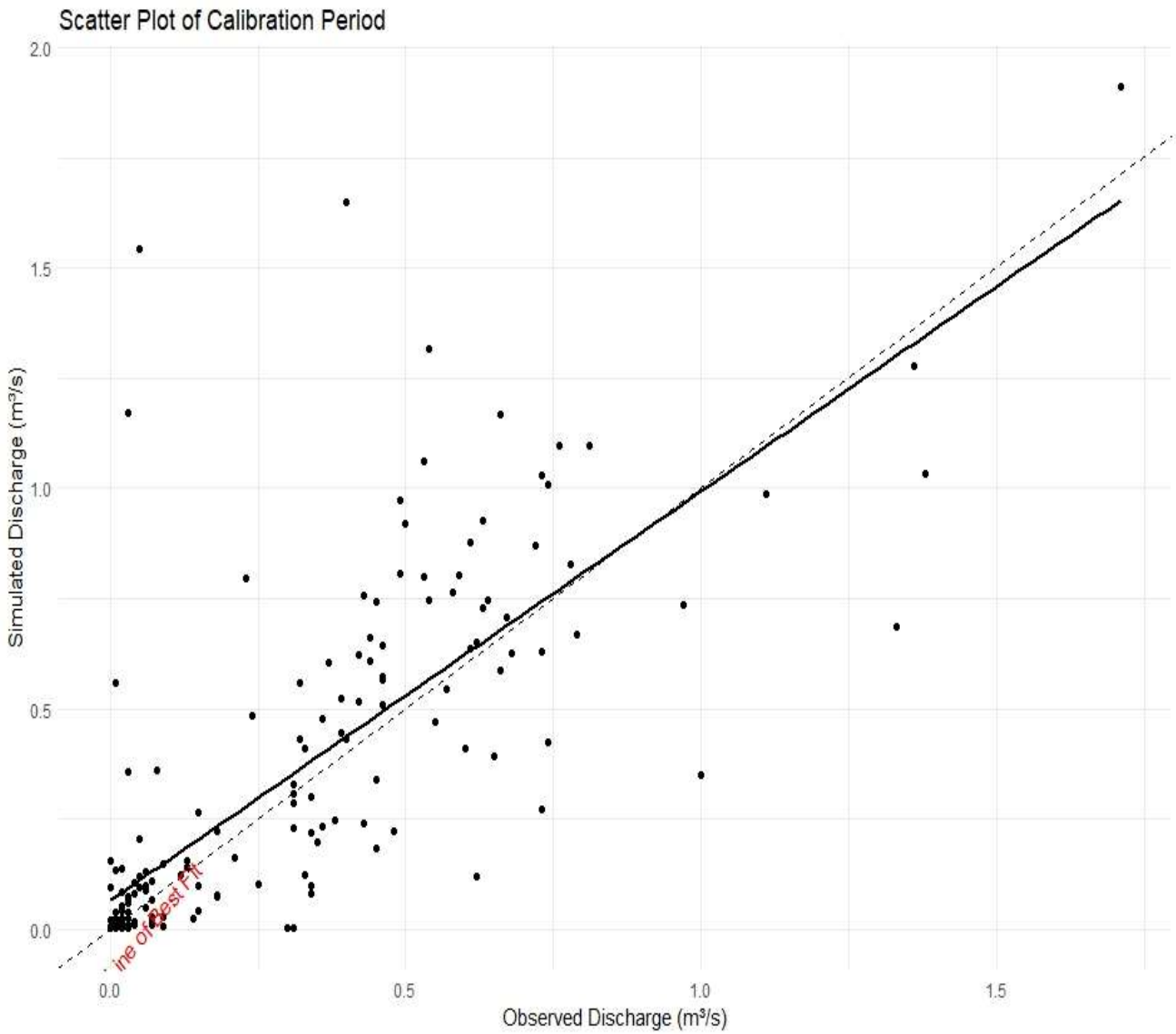

Figure 24: Scatter plot of the observed and simulated monthly average flow (m3/s) in the calibration phase.

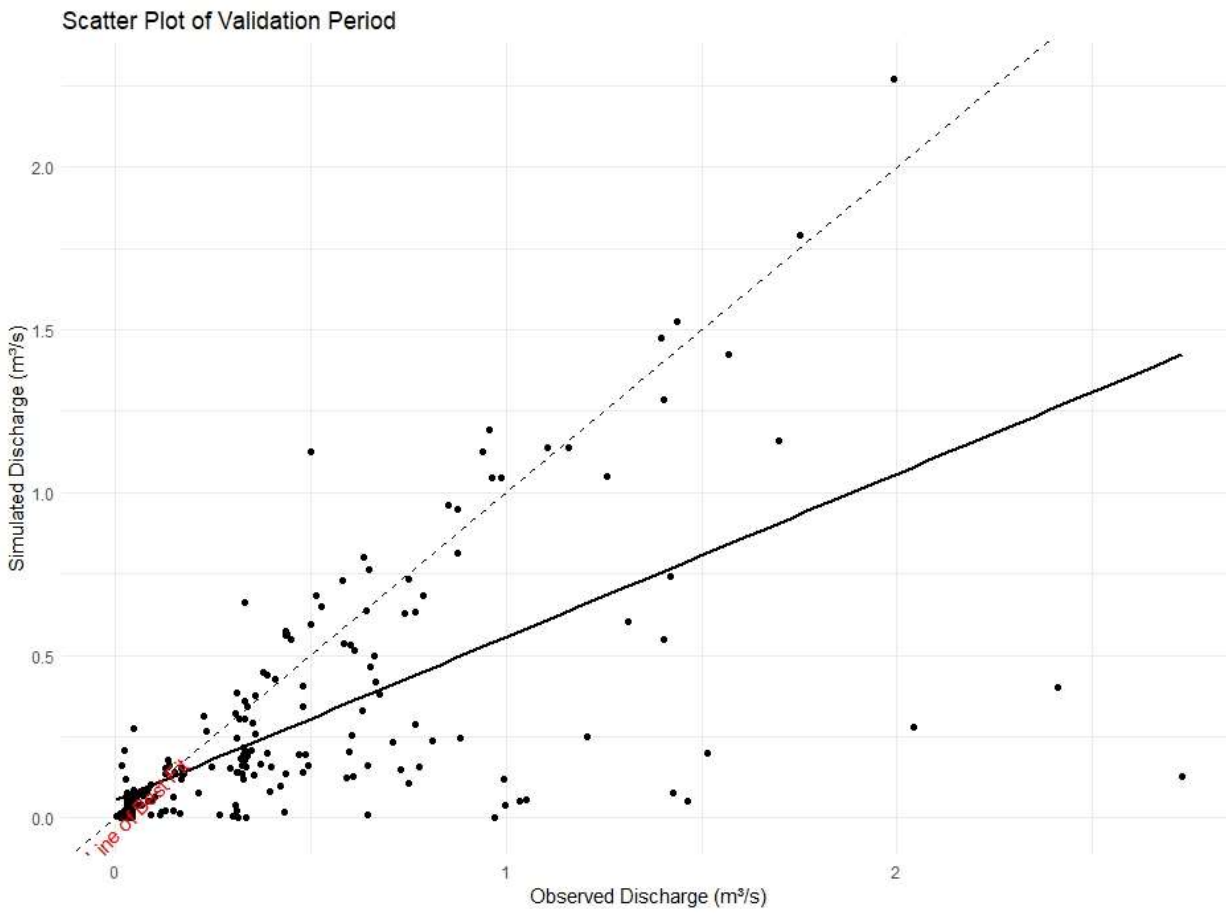

Figure 25: Scatter plot of the observed and simulated monthly average flow (m3/s) during the validation period.

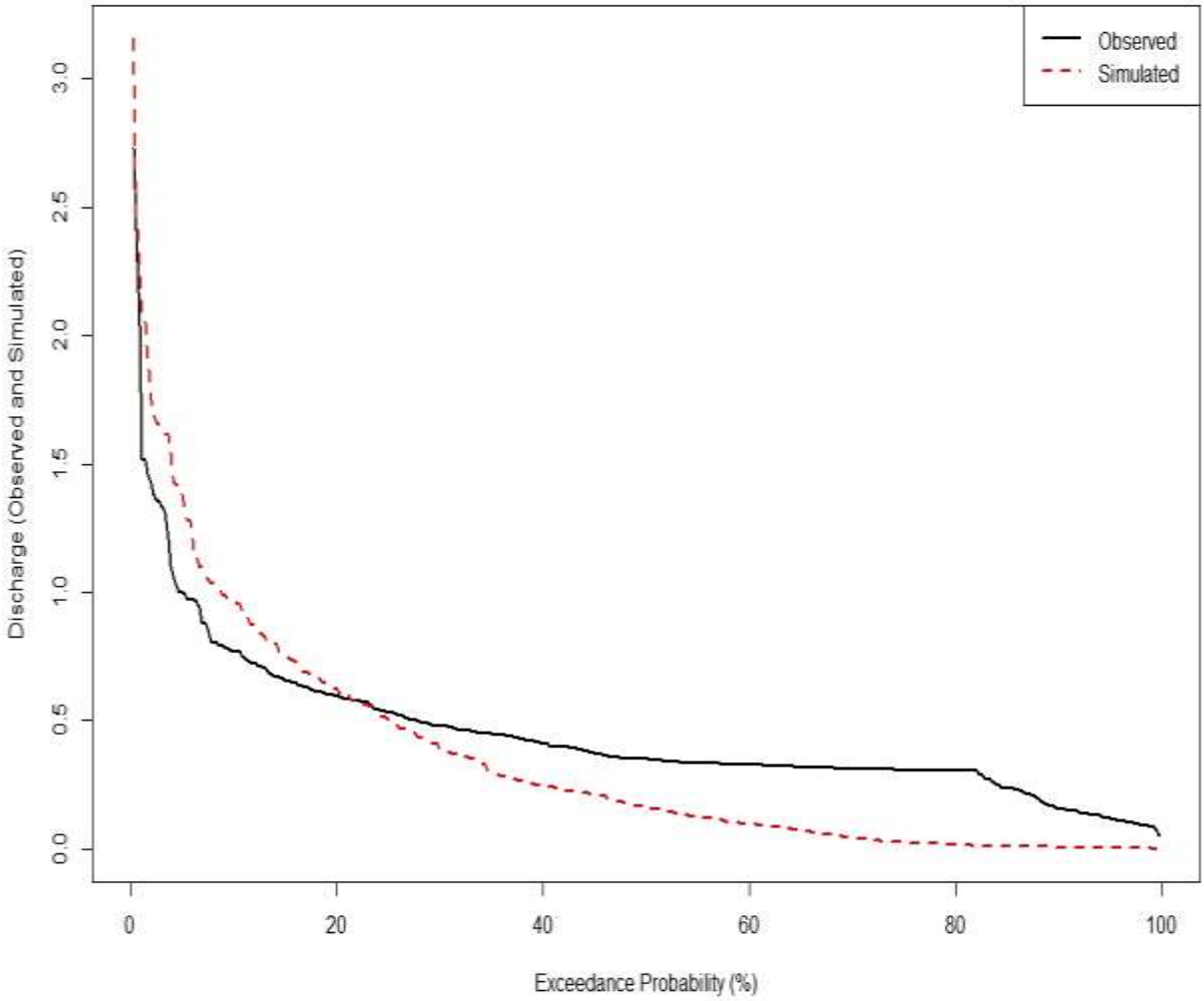

Figure 26: Flow Duration Curve of Observed and Simulated Discharge of Mulunguzi River Basin

4.3.3 Impacts of Land Use and Climate Changes on Streamflow

The SWAT model simulated various water balance components under specific scenarios in this research. Surface runoff, base flow, water yield, and evapotranspiration were the primary focus of this study. A similar study was conducted in Ethiopia's Birr River Watershed, Abbay Basin by Malede et al. (2022) with a comparable emphasis.

4.3.3.1 Hydrological Effects of LULC

Table 9 presents the results of two scenarios (Sc) that illustrate how LULC alterations affect the MRB's hydrological response. Sc2 used the LULC map for 2000, while Sc3 used the map for 2020. Both scenarios were coupled with baseline climate data from 1990-1997. The SWAT model output shows that surface runoff decreased by 1.28% in Sc2 but increased by 119.9% in Sc3. Baseflow reduction was observed in both scenarios, with a decrease of 1.4% in Sc2 and 17.8% in Sc3. There was also a decrease in evapotranspiration in Sc2 and Sc3, at 0.06% and 4.6% respectively. Water yield increased in both scenarios, by 0.06% and 2.9% respectivelyThe SWAT model output revealed a decrease in surface runoff by -1.28% in Sc2, but an increase of 119.9% in surface runoff was found in Sc3. Baseflow reduction was observed in Sc2 and Sc3, with a decrease of -1.4% and -17.8%, respectively. There was also a decrease in evapotranspiration in Sc2 and Sc3, at -0.06% and -4.6%, respectively. The student’s T-test demonstrated a significant increase in surface runoff and a reduction in baseflow in Sc3, indicating a clear manifestation of LULC alteration that occurred in the MRB between 2000 and 2020. Table 4 shows that forest land was reduced by -16 %, and bare land increased by 8.7% during this period, significantly contributing to the 23% cumulative reduction in forest land and 11.8% increase in bare land from 1990 to 2020. When forested land is converted into cultivated or bare land, the soil's ability to retain water decreases. This leads to a decrease in baseflow and an increase in surface runoff, which ultimately results in higher water yield. A similar observation was made in Ethiopia's Keleta watershed by Bekele et al. (2021). They discovered that the expansion of cultivated lands and the reduction of ground cover resulted in an increase in surface runoff and a decrease in baseflow. The study also found that the reduction in forested areas resulted in reduced evapotranspiration. These changes in LULC contributed to higher runoff rates by decreasing surface roughness, which in turn increases flow velocity and reduces infiltration. The findings in Sc3 show an increase in water yield, which is

consistent with the research conducted by Measho et al. (2020) in the Mareb-Gash River Basin located in the Horn of Africa. The study also discovered that a reduction in forested areas significantly contributed to the increased water yield in all the catchments. LULC changes directly influence the hydrological components of a basin by altering the physical processes of water movement and storage (Achugbu et al., 2022). The findings on the hydrological effects of LULC changes in the MRB align with those of Nkhoma et al. (2021). The study reported a 16.56% rise in stream flow in the Wankurumadzi River Basin between the 1990s and the 2000s due to LULC changes. Another study by Kambombe (2018) on the Thondwe watershed noted a similar increase in runoff by 2.9%. This increase was a result of a -19% reduction in forest land and an increase in cultivated and bare land at 11% and 15%, respectively, between 1973 and 1994.

4.3.3.2 Hydrological Impacts of Climate Change

In order to assess the impact of climate change on the hydrology of the MRB, two scenarios were created, Sc4 and Sc5. The LULC data was consistent with the baseline, while the climate data varied between 1998-2008 and 2009-2020. The data presented in Table 10 indicates that scenario 5 (Sc5) experienced a significant surface runoff increase of 152.2%, while scenario 4 (Sc4) saw a decrease of -22.8%. Both Sc4 and Sc5 experienced an increase in baseflow, with Sc5 showing a more significant rise of 33.6% compared to 8.2% in Sc4. The increase in evapotranspiration was also observed in both scenarios, but Sc5 showed a more considerable increase of 59.4% compared to 9.1% in Sc4. Additionally, water yield increased in both Sc4 and Sc5, by 2.78% and 51.11%, respectively. Sc5, as represented in Figure 14, covers the period of 2010s and 2020s. During this time, there was an increase in both rainfall and temperature as compared to Sc4. This increase in rainfall led to higher surface runoff, baseflow, and water yield in the MRB. Furthermore, the rise in temperature resulted in an increase in evapotranspiration, which was further compounded by the increase in rainfall. These findings are consistent with the results from the research conducted by Ndhlovu and Woyessa (2020) on the Kabompo River in the Zambezi River Basin. The study examined two Representative Concentration Pathways (RCP 4.5 and RCP 8.5) scenarios and found that under RCP 8.5, there was a higher surface runoff, baseflow, evapotranspiration, and water yield than under RCP 4.5. The study also explained that under RCP 8.5, extreme precipitation events may become more frequent compared to RCP 4.5. In a similar study by Worqlul et al. (2018), it was projected that in the Headwater Catchments of the Upper Blue Nile Basin in

Ethiopia, there will be a 64% increase in streamflow in the dry season and a 19% decrease in the wet season by the end of the 21st Century. This was attributed to increased rainfall events during the dry season than the wet season. The findings also revealed a consistent increasing trend in temperature which will be responsible for the increased evapotranspiration by 7.8% by the end of the century. According to a study conducted by Adhikari & Nejadhashemi in 2016, Malawi is expected to experience a temperature rise of 1.6°C-2.9°C and a precipitation increase of 1.8%-24.6% between the 1990s and 2050s as a result of climate change. The study specifically found that the Lake Chilwa basin will experience a 1.4% increase in evapotranspiration, an 8.2% increase in surface runoff, and a 7.9% increase in water yield due to these changes. The study's findings align with the results in the MRB, which is a subbasin within the Lake Chilwa Basin.

4.3.3.3 The Hydrological Impacts of LULC and Climate Change

To analyze the hydrological response of the Mulunguzi watershed to the impact of changes in LULC and CC, the LULC map of 2000 was used along with climate data from 1998 to 2008. The LULC map of 2020 was also used with climate data from 2009 to 2020. In Table 11, the results show a pronounced increase in runoff of 303.8% between the baseline and Sc7. This increase in runoff is due to the highest amount of rainfall recorded between the 2010 and 2020 decades, compounded by the reduction in forest land and increased bare land during the same period. Base flow increased by 17.2%, Evapotranspiration decreased by 2.8%, and water yield increased by 71%. The Mulunguzi watershed's hydrological response to the combined effects of LULC and CC is greater than the individual effects. Under Sc6, surface runoff decreased by -27%, baseflow increased by 2.8%, a reduction in evapotranspiration by -0.04%, and increase in water yield by 0.06%. The explanation is based on the slight change in forested areas from 46.97% to 40.04% between 1990 and 2000. In addition, the grassland area increased by 10.47% over the same period. This explains the decrease in runoff with a slight increase in base flow despite climate change playing its role. The considerable increase in runoff during recent years indicates a significant change in LULC between 2000 and 2020, combined with intense and frequent rainfalls caused by climate change. Both LULC and CC significantly impact the hydrological components of the MRB. Several other watersheds have shown comparable findings to the ones mentioned. For instance, in the Abbay Basin of Ethiopia, Malede et al. (2022) discovered that the combined impacts of LULC and CC have a more significant effect on surface runoff than their individual effects. As a result,

surface runoff increased by 90.07%, baseflow increased by 14.62%, and evapotranspiration decreased by -1.9% between 1997 and 2007. A study conducted by Aboelnour et al. (2019) in Little Eagle Creek of Indiana found that the combined impacts of land use and climate change had a more significant effect on changes in water yield than the separate impacts of either factor. As a result of the combined impacts, water yield increased by 20%. The study also showed that although climate change played a dominant role in the increase of water yield by 17.9% compared to land use by 6.7%, the growth of urban areas led to an increase in surface runoff and a decrease in baseflow. Land use change resulted in a 28.8% reduction in baseflow, while climate change led to a 15.2% increase. When both factors were combined, the baseflow reduced by 23%.

Table 9 Mean monthly hydrological components for the effect of land use.

Scenario (Impact Of LULC)	LULC	Climate	Surface Runoff (mm)	Change (mm)	Change (%)	Base flow (mm)	Change (mm)	Change (%)	Evapotranspiration (mm)	Change (mm)	Change (%)	Water Yield (mm)	Change (mm)	Change (%)
Sc1	1990	1990-1997	7.84			30.45			32.22			49.94		
Sc2	2000	1990-1997	7.74	-0.1	-1.28	30.02	-0.4	-1.4	32.2	-0.02	-0.06	49.97	0.03	0.06
Sc3	2020	1990-1997	17.24	9.4	119.9	25.05	-5.4	-17.8	30.73	-1.5	-4.63	51.37	1.4	2.86

Table 10 Mean monthly hydrological components for the effect of climate change.

Scenario (Impact Of LULC)	LULC	Climate	Surface Runoff (mm)	Change (mm)	Change (%)	Base flow (mm)	Change (mm)	Change (%)	Evapotranspiration (mm)	Change (mm)	Change (%)	Water Yield (mm)	Change (mm)	Change (%)
Sc1	1990	1990-1997	7.84			30.45			32.22			49.94		
Sc4	1990	1998-2008	6.05	-1.8	-22.8	32.96	2.5	8.24	35.12	2.9	9.1	51.33	1.4	2.78
Sc5	1990	2009-2020	19.77	11.9	152.2	40.71	10.2	33.64	51.33	19.1	59.37	75.47	25.5	51.11

Table 11 Mean hydrological components for the LULC and climate change combined effect.

Scenario (Impact Of LULC)	LULC	Climate	Surface Runoff (mm)	Change (mm)	Change (%)	Base flow (mm)	Change (mm)	Change (%)	Evapotranspiration (mm)	Change (mm)	Change (%)	Water Yield (mm)	Change (mm)	Change (%)
Sc1	1990	1990-1997	7.84			30.45			32.22			49.94		
Sc6	2000	1998-2008	5.7	-2.1	-27.3	31.31	0.9	2.83	32.18	-0.04	-0.13	49.97	0.03	0.06
Sc7	2020	2009-2020	31.69	23.8	303.8	35.71	5.3	17.24	31.31	-0.9	-2.82	85.52	35.6	71.23

CHAPTER 5

CONCLUSIONS AND RECOMMENDATIONS

5.1. Conclusions

The study analyzed changes in LULC in the MRB from 1990 to 2020. The study also assessed the individual and combined impacts of LULC and CC on the streamflow of the Mulunguzi River in Zomba. By utilizing the SWAT model, the study investigated the hydrological response of the Mulunguzi watershed to the impacts of LULC and CC. The results of the study confirm that:

- ✓ There was a reduction in forest land by 23 % between 1990 and 2020. On the other hand, agricultural land, bare land, and grassland increased by 4.7%, 11.82%, and 8.66%, respectively, during the period.
- ✓ The hydro-climatic analysis showed an increase in the mean monthly and annual temperatures by 0.004°C per month and 0.041°C per year, respectively. This was caused by a significant increase in minimum temperatures at both monthly and annual timescales. A non-significant decreasing trend was observed in the monthly and annual series for the maximum temperatures.
- ✓ The study found an increasing trend in rainfall at 4.92mm per year from 1990 to 2020. However, this annual increase was not statistically significant. There was a slightly increasing annual rainfall trend in the 1990s compared to the 2000s and the 2010s. However, the 2010s recorded the highest rainfall, followed by the 2000s. This was attributed to high rainfall events in 2017, 2018, and 2019. The lowest rainfall events were observed in 1990 and 1995. The 2010s received the highest amount of rainfall.
- ✓ Results of the calibration and validation of the SWAT model indicated that the model could simulate the hydrological responses of the Mulunguzi watershed under different LULC and climate change scenarios.

- ✓ Changes in LULC resulted in a 119.9% increase in surface runoff and a 2.9% increase in water yield. However, it caused a decrease of -17.8% in baseflow and -4.6% in evapotranspiration. On the other hand, CC alone caused a 152.5% increase in surface runoff, a 33.6% increase in baseflow, a 59.3% increase in evapotranspiration, and a 51% increase in water yield. When LULC and CC were combined, there was a 303.8% increase in surface runoff, a 17.24% increase in baseflow, and a 71% increase in water yield. However, evapotranspiration decreased by -2.8%.

The LULC changes in the MRB from 1990 to 2020 have led to the conversion of forested areas to bare or agricultural lands. This conversion has increased surface runoff and reduced infiltration, thereby affecting the flow of the Mulunguzi River and reducing the availability of water in the catchment. Additionally, higher rainfall and temperatures have resulted in increased surface runoff, baseflow, evapotranspiration, and water yield in the catchment. When LULC changes and CC are combined, the resulting impact is worse than the individual effects of either. Therefore, it can be inferred that the Mulunguzi River's flow is significantly influenced by the combined effects of LULC and CC. These findings indicate a negative impact on the availability of water within the MRB for various uses, including water supply. Therefore, the study quantified the impacts of two environmental factors affecting hydrological processes in the MRB. This provides an opportunity to develop climate change mitigation measures and catchment management strategies.

5.2. Recommendations

The scope of this study was limited, leaving areas for improvement or extension. Based on the conclusions drawn from this research, it is recommended that:

- ✓ An additional study should be conducted using different models to determine whether the hydrological response of the MRB to changes in LULC and CC will differ from that of the SWAT output.
- ✓ The SWAT model should be applied robustly in all Lake Chilwa Basin sub-basins to determine if this study's results are specific to the MRB.
- ✓ Further studies should consider future climatic conditions and LULC changes to assess future water availability in the MRB.
- ✓ Natural Based Solutions should be employed in the management of the Mulunguzi Catchment to mitigate the combined impacts of LULC change and CC.

REFERENCES

Achugbu, I. C., Olufayo, A. A., Balogun, I. A., Dudhia, J., McAllister, M., Adefisan, E. A., & Naabil, E. (2022). Potential effects of Land Use Land Cover Change on streamflow over the Sokoto Rima River Basin. *Heliyon*, *8*(7), e09779. https://doi.org/10.1016/j.heliyon.2022.e09779

Arora, V. K., & Boer, G. J. (2001). Effects of simulated climate change on the hydrology of major river basins. *Journal of Geophysical Research: Atmospheres*, *106*(D4), 3335–3348. https://doi.org/10.1029/2000JD900620

Bekele, D., Alamirew, T., Kebede, A., Zeleke, G., & Melesse, A. M. (2021). Modeling the impacts of land use and land cover dynamics on hydrological processes of the Keleta watershed, Ethiopia. *Sustainable Environment*, *7*(1), 1947632. https://doi.org/10.1080/27658511.2021.1947632

Cassivi, A., Tilley, E., Waygood, E. O. D., & Dorea, C. (2020). Trends in access to water and sanitation in Malawi: Progress and inequalities (1992–2017). *Journal of Water and Health*, *18*(5), 785–797. https://doi.org/10.2166/wh.2020.069

de Wit, M., & Stankiewicz, J. (2006). Changes in Surface Water Supply Across Africa with Predicted Climate Change. *Science*, *311*(5769), 1917–1921. https://doi.org/10.1126/science.1119929

Deng, Z., Zhang, X., Li, D., & Pan, G. (2015). Simulation of land use/land cover change and its effects on the hydrological characteristics of the upper reaches of the Hanjiang Basin. *Environmental Earth Sciences*, *73*(3), 1119–1132. https://doi.org/10.1007/s12665-014-3465-5

Dias, J. L. (2008). *Assessment of impacts of socio-economic activities on water quality within Mulunguzi Catchment (Master's Thesis).* University of Zimbabwe.

Fant, C., Gebretsadik, Y., McCluskey, A., & Strzepek, K. (2015). An uncertainty approach to assessment of climate change impacts on the Zambezi River Basin. *Climatic Change*, *130*(1), 35–48. https://doi.org/10.1007/s10584-014-1314-x

Gashaw, T., Tulu, T., Argaw, M., & Worqlul, A. W. (2018). Modeling the hydrological impacts of land use/land cover changes in the Andassa watershed, Blue Nile Basin, Ethiopia. *Science of The Total Environment*, 619–620(1), 1394–1408. https://doi.org/10.1016/j.scitotenv.2017.11.191

Gautam, M. (2006). *Managing Drought in Sub-Saharan Africa: Policy Perspectives*. http://doi.org/10.22004/ag.econ.25608

Hamududu, B., & Killingtveit, Å. (2016). Hydropower Production in Future Climate Scenarios; the Case for the Zambezi River. *Energies*, *9*(7). https://doi.org/10.3390/en9070502

Jensen, J. R. (2015). *Introductory Digital Image Processing: A Remote Sensing Perspective*. Pearson.

Mbano, D., Chinseu, J., Ngongondo, C., Sambo, E., & Mul, M. (2009). *Impacts Of Rainfall And Forest Cover Change On Runoff In Small Catchments: A Case Study Of Mulunguzi And Namadzi Catchment Areas In Southern Malawi*. Malawi Journal of Science & Technology, 9(1), 11-17.

Meins, F. M. (2013). *Evaluation of spatial scale alternatives for hydrological modelling of the Lake Naivasha basin, Kenya* (Master's thesis). University of Twente

Mengistu, D., Bewket, W., Dosio, A., & Panitz, H.-J. (2021). Climate change impacts on water resources in the Upper Blue Nile (Abay) River Basin, Ethiopia. *Journal of Hydrology*, *592(* 125614). https://doi.org/10.1016/j.jhydrol.2020.125614

Ngongondo. (2005). An Analysis of Long Term Rainfall Variability, Trend and Water Availability In Mulunguzi River Catchment Area, Zomba, Malawi. *Malawi Journal of Sci and Techn.,* 7(1),34-44

Ngongondo, C., Xu, C.-Y., Gottschalk, L., & Alemaw, B. (2011). Evaluation of spatial and temporal characteristics of rainfall in Malawi: A case of data scarce region. *Theoretical and Applied Climatology*, *106*(1–2), 79–93. https://doi.org/10.1007/s00704-011-0413-0

Nhemachena, C., Nhamo, L., Matchaya, G., Nhemachena, C. R., Muchara, B., Karuaihe, S. T., & Mpandeli, S. (2020). Climate Change Impacts on Water and Agriculture Sectors in Southern Africa: Threats and Opportunities for Sustainable Development. *Water*, *12*(10). https://doi.org/10.3390/w12102673

Nkhoma, L., Ngongondo, C., Dulanya, Z., & Monjerezi, M. (2021). Evaluation of integrated impacts of climate and land use change on the river flow regime in Wamkurumadzi River, Shire Basin in Malawi. *Journal of Water and Climate Change*, *12*(5), 1674–1693. https://doi.org/10.2166/wcc.2020.138

Poff, N. L., Allan, J. D., Bain, M. B., Karr, J. R., Prestegaard, K. L., Richter, B. D., Sparks, R. E., & Stromberg, J. C. (1997). The Natural Flow Regime. *BioScience*, *47*(11), 769–784. https://doi.org/10.2307/1313099

Tesfaye, G., Assefa, A., & Kidane, D. (2017). Runoff, sediment load and land use/cover change relationship: The case of Maybar sub-watershed, South Wollo, Ethiopia. *International*

Journal of River Basin Management, *15*(1), 89–101. https://doi.org/10.1080/15715124.2016.1239625

Westerberg, I. K., Guerrero, J.-L., Younger, P. M., Beven, K. J., Seibert, J., Halldin, S., Freer, J. E., & Xu, C.-Y. (2011). Calibration of hydrological models using flow-duration curves. *Hydrology and Earth System Sciences*, *15*(7), 2205–2227. https://doi.org/10.5194/hess-15-2205-2011

Worqlul, A., Dile, Y. T., Ayana, E., Jeong, J., Adem, A., & Gerik, T. (2018). Impact of Climate Change on Streamflow Hydrology in Headwater Catchments of the Upper Blue Nile Basin, Ethiopia. *Water*, *10*(2). https://doi.org/10.3390/w10020120

APPENDICES

APPENDIX A

A1: Lookup table for LULC

lookuptablelulc.txt - Notepad

File Edit Format View Help

```
"VALUE","LANDUSE"
1,FRSE
154,FRST
204,AGRL
219,WATR
225,BARR
```

A2: Lookup table for Soil map

soil.txt - Notepad

File Edit Format View Help

```
"VALUE","NAME"
644,I-Bc-c-644
```

APPENDIX B

B 1: Final HRU Distribution Report

HRULandUseSoilsReport.txt - Notepad

File Edit Format View Help

```
SWAT   model  simulation   Date: 7/30/2023 12:00:00 AM   Time: 00:00:00
MULTIPLE HRUs  LandUse/Soil/Slope OPTION             THRESHOLDS : 10 / 5 / 5 [%]
Number of HRUs: 275
Number of Subbasins: 31

                                                     Area [ha]          Area[acres]

Watershed                                            1792.7100            4429.8760

                                                     Area [ha]          Area[acres] %Wat.Area
LANDUSE:
                        Forest-Evergreen --> FRSE    1030.8035            2547.1670     57.50
                            Forest-Mixed --> FRST     527.4155            1303.2700     29.42
                Agricultural Land-Generic --> AGRL    148.3776             366.6485      8.28
                                   Barren --> BARR     86.1134             212.7905      4.80

SOILS:
                                   I-Bc-c-644        1792.7100            4429.8760    100.00

SLOPE:
                                        10-15         312.4964             772.1942     17.43
                                         7-10         142.8181             352.9106      7.97
                                          5-7          46.9334             115.9747      2.62
                                      15-9999        1222.0888            3019.8425     68.17
                                          0-5          68.3734             168.9540      3.81
```

APPENDIX C

C 1: Input file for precipitation data

pp.txt - Notepad

File Edit Format View Help

```
ID,NAME,LAT,LONG,ELEVATION
1,Kuchawe,35.3000,-15.3000,1800
2,Makoka,35.1500,-16.5000,580
3,Chanco,35.3380,-15.3885,888
```

C 2: Input file for temperature data

temp.txt - Notepad

File Edit Format View Help

```
ID,NAME,LAT,LONG,ELEVATION
1,Kuchawe,35.3000,-15.3000,1800
2,Makoka,35.1500,-16.5000,580
3,Chanco,35.3380,-15.3885,888
```